TECHNICAL PAPER

Influence of rice husk ash (RHA) with gypsum and ichu fibers in the processing of geopolymers

Sócrates Pedro Muñoz Pérez[1,2] · Samuel Charca Mamani[3] · Luigui Italo Villena Zapata[4] · Jorge Luis Leiva Piedra[5] ·
Simon Gonzales Ayasta[6] · Ernesto Dante Rodriguez Lafitte[6] · Fidel Gregorio Aparicio Roque[7] ·
Omar Coronado Zuloeta[8]

Abstract

Cement production consumes enormous amounts of fossil fuels, generating significant CO_2 emissions, seriously impacting the environment, and tons of rice husk ash (RHA) are generated annually as a result of energy production activities, much of which goes unused and is deposited in landfills, causing serious environmental damage. The present research aims to study the mechanical and microstructural properties of geopolymer with RHA, gypsum and ichu fiber, with alkaline activators of sodium hydroxide and sodium silicate. Geopolymers at 8, 10, 12 and 14 molar of sodium hydroxide with proportions of 10, 20, 30, 40 and 50% of gypsum and 0.5, 1.0, 1.5 and 2.0% of ichu fiber were elaborated and subjected to mechanical strength and microstructure analysis. The results revealed that the best combination was 12 molar with 20% gypsum and 1.5% ichu fiber, with compressive, flexural and tensile strengths of 9.72, 7.99 and 2.25 MPa; respectively, SEM images showed the generation of a large amount of geopolymeric products by the reaction of OH with the aluminosilicate components of the RHA in an alkaline source. XRD shows as crystalline phases albite, quartz, orthoclase, aphthalite and also amorphous crystalline phase. FTIR spectra showed related to H–O–H and O–H stretching vibrations of broad bands around $3450 \, cm^{-1}$, thermogravimetric analysis shows that the residual mass at the end of the test at 990 °C is 90.6%. It is concluded that sodium hydroxide, sodium silicate together with RHA, gypsum and ichu fibers can be used as reactive materials to produce geopolymers with good mechanical characteristics.

Keywords Ichu fiber · Rice husk ash · Gypsum · Mechanical properties · Microstructure · Geopolymer

Introduction

Tun et al. [1], state that the development of the world's major economies accompanied with population growth, has led to a progressive increase in the use of building materials making the demand for cement and its industry consumes a large amount of fossil fuels to carry out the production of cement, is contrasted by Ali et al. [2], stating that the cement industry alone consumes almost 12 to 15% of total industrial energy use, emitting approximately 7% of carbon dioxide and cement production also consumes primary energy, which is approximately 3% of the world consumption [3] generating severe environmental impact estimated that to produce 1000 kg of cement will emit 1000 kg of CO2 as stated by Shehata et al. [4] and that according to Babaee and

Castel [5] the world demand for cement will grow up to 5.5 GTon per year by 2050.

Cement-based building materials decompose easily at temperatures above 500 °C, so environmentally friendly and high temperature resistant materials are needed, for this reason geopolymers are considered and evaluated for application as refractory and high thermal insulation materials due to their superior thermal properties, such as the ability to set quickly with high ultimate compressive strength when they have optimal amounts of calcium [6], for this reason, gypsum was added in this study so that it can help the geopolymer to set quickly due to the calcium content of gypsum.

The possibility of using cementitious by-products such as blast furnace slag, fly ash (FA), silica fume and for the production of cement-free concrete is necessary to mitigate the negative impact on the environment, making it an ecofriendly and sustainable material [7, 8], that is why the production of cement-free geopolymer concrete is a promising

technology [9] where the utilization of 100% of industrial and agro-industrial waste to produce alkali-activated materials is going to result in geopolymers, which are sustainable and environmentally friendly materials that have unique engineering properties, good durability against different chemical and physical aggressive agents, thermally stable, easy to work with, environmentally friendly, emit low levels of CO_2 emissions and do not require high industrial energy consumption for their manufacture [10, 11] as it results from mixing an amorphous 3D structure with aluminosilicate materials [12]. The starting materials contain a huge content of SiO_2 and Al_2O_3 such as FA, metakaolin (MK), rice husk ash (RHA) which are activated by strong alkaline solutions like NaOH or KOH [13].

On the other hand, huge amounts of RHA are generated every year, most of which are not used or are disposed of in landfills, resulting in severe environmental degradation. To avoid this, the use of RHA as precursors or coagents in the development of alkali-activated materials is considered a viable alternative to alleviate the environmental problems associated with the disposal of RHA [14, 15]. For RHA to be an extremely pozzolanic material, it is necessary to have the combustion temperature under control, for this it is necessary to perform compressive strength tests to evaluate the pozzolanic activity and thus have better mechanical strength results when substituting RHA for cement in the production of concrete [16], which is why the heat treatment of RHA improves the pozzolanic performance by reducing the loss on ignition. Rithuparna et al. [17], mentions that the optimum combustion temperature of RHA ranges from 500 to 700 °C, and also states that the grinding of ashes helps to increase its pozzolanic activity index, which would be above 75%, registering an improvement in compressive strength between 10 and 50%.

The aforementioned can also be verified with Newaz et al. [18] and Mohd et al. [19], stating that to obtain the desired properties of the RHA, a controlled combustion and a good crushing is essential, it is complicated to obtain 100% RHA in the reactive form of amorphous silica since part of the ash is converted into crystalline phase where the incorporation of the incinerated RHA has a significant effect on the properties of the geopolymer. The optimum burning temperature helps to develop the highest amount of silica as stated by Anjani et al. [20], mentioning that the RHA is composed in percentage with respect to its total mass of the following chemical compounds, 95.60% of silica (SiO_2), 0.20% of magnesium oxide (MgO), 0.30% of calcium oxide (CaO) and 1.20% of iron oxide (Fe_2O_3), with silica standing out as the compound with the highest percentage, however, for burn temperatures between 500 and 700 °C of the RHA the amount of silica decreases to 86.76% and for the other compounds the percentages would be: 0.0038% of Al_2O_3, 2.468% of CaO and 0.887% of MagO [21, 22]. The high

percentage of silica in the RHA causes the setting time of the geopolymer to increase, so it is necessary to treat the geopolymer with materials that have calcium in their composition, as is the case of gypsum.

Geopolymers are significantly lighter than conventional concrete with made with Portland cement, according to the study by Öztürk [23] manifests that 12 molar (M) geopolymers, have an average unit weight of 1535 kg/m^3 and 1692 kg/m^3 with a SS/SH ratio of 2 and 2. 5, respectively, but what investigated by Alsaif et al. [24], indicate that the average unit weight of geopolymer is 2134 kg/m^3, similar results obtained by researchers Topçu and Sofuoğlu [25] whose average unit weights of geopolymers are 1950 kg/m^3, on the other hand, the unit weight of conventional concrete is major and ranges from 2437.53 to 2469.14 kg/m^3 [26]. Another physical property such as air content is also important to measure, for the case of the study conducted by Kotop et al. [27] the air content of the elaborated geopolymers varied between 2.4 and 3.4%, in another research the air content varies between 1.5 and 1.70% as mentioned by researchers Saloni et al. [28].

According to a study carried out by Somna et al. [13], RHA can be used in the production of geopolymers, allowing it to replace FA up to 50%, obtaining compressive stress of 4.1 MPa at 28 days, which contrasts with the results of Lianasari et al. [29] who elaborated geopolymers based on FA:RHA in proportions of 60:40; 40:60 whose results were 7.09 MPa, 4.08 MPa, respectively. However, according to Hossain et al. [30], when evaluating the influence of RHA on the geopolymer, adding 10–20% of the total weight, RHA significantly improves the properties of the geopolymer in the short and long term, this result is slightly different from that obtained by Chao-Lung and Trong-Phuoc [31] indicating that the specimens prepared with a concentration of NaOH at 10 M and 35% RHA had the highest compressive strength and that as the molarity of NaOH and the amount of RHA increased above these values, the compressive strength decreased and the chemical analysis showed that the main crystalline phases present in the resulting geopolymer were quartz, mullite and cristobalite, in addition, minor zeolite phases were detected in all geopolymer samples. According to the results obtained for geopolymers made from RHA, their mechanical strength at 28 days is not high, as is the case for geopolymers made from blast furnace slag and fly ash, which are wastes containing calcium in their chemical composition.

The incorporation of RHA also yielded positive results in the research conducted by Zabihi et al. [32] a slight increase in the compressive stress of the geopolymer is observed up to 3.6% in the 100% RHA and 0.5% polypropylene fiber blend, the improvement is a product of the interaction between the fibers and the macro- and micro-cracks since as the pioneer cracks move toward the fibers, the matrix

interface deflects the crack path and then the concrete with fibers sustains additional compressive load, leading to an increase in compressive stress. But it is not only the RHA that improves the mechanical strength of a geopolymer but also the NaOH concentration, as evidenced in the research conducted by Januar et al. [33] whose results showed that geopolymers made at 12, 14, 16 and 18 M NaOH obtained compressive strength tests of 9.87, 10.93, 12.0 and 14 MPa, respectively, concluding that increasing the molarity of NaOH improves the compressive strength of the geopolymer. While it is true that increasing the molarity of NaOH in the mixture of geopolymer with rice husk ash will increase the mechanical strength, it is also necessary to study how gypsum will influence the increase in NaOH molarity.

The opposite was the case in the research conducted by Handayani et al. [34], who fabricated geopolymers with sodium silicate and sodium hydroxide at 8, 10 and 12 molar (M), with the result that the mixture of 10 M NaOH with sodium silicate improved the compressive stress by 16.21% and the flexural stress and fracture toughness by 81.6%; however, sodium silicate combined with 12 M NaOH reduced the compressive stress by 13.6%, 21% and flexural strength and fracture toughness by 81.6%, however, sodium silicate combined with 12 M NaOH reduced compressive strength by 13.23% and flexural strength and fracture toughness by 61.94%., evidencing that not necessarily increasing the molarity of sodium hydroxide increase the mechanical strength.

It is necessary to indicate that the higher the concentration of RHA, the longer the setting time, as mentioned by Rosyadi [35] who elaborated a geopolymer of FA and RHA in proportions of 100:0, 95:5, 90:10 and 85: 15, in the first mixture has a compressive strength that complies with the regulations, but the setting time is too fast, while in those used with 5% and 10% RHA substitution has a higher compressive strength and can increase the setting time, but the addition of 15% RHA makes the setting time too long and reduces the compressive stress, this is due to the high calcium content in fly ash type C which produces significantly high compressive strength, but has a fast setting time, RHA absorbs a huge amount of water and contains a high content of silica oxide to delay the setting time and decreasing the compressive strength, similar results obtained Ilmiah when producing geopolymers based on FA and RHA at 100: 0, 50:50 and 0:100% obtained compressive tests of 43.32 MPa, 7.65 MPa and 2.58 MPa, respectively, indicating that RHA can potentially increase the setting time because it stores water in its cavity and requires a lot of water for mixing, but it decreases the compressive strength of the geopolymer [36], Therefore, RHA with a high silica content is a material with suitable characteristics to manufacture an alkaline activator having RHA as a precursor material that can be used to produce geopolymers [37].

On the other hand what investigated by An et al. [38] who fabricated geopolymers containing 0%, 5%, 10% recycled gypsum and 60%, 70%, 80% soda residue by dry weight as a partial substitute for granulated blast furnace slag, the test results reveal that the strength-based geopolymer decreases with increasing dosage and increases with increasing curing age and an excessive dosage of 10% recycled gypsum as a partial substitute for GGBS was detrimental to the strength of geopolymer, while a dosage of 5% was beneficial in increasing the compressive strength value to 9.31 MPa [38], similar case happened in the research conducted by Cong and Mei [39] who elaborated geopolymers with fly ash, granulated blast furnace slag and calcium carbide residues, adding gypsum as a supplementary activator in all geopolymer binders, and the gypsum dosage was 5 wt% of the aluminosilicate precursor reaching compressive strengths of 30 MPa.

The use of natural fibers in the production of geopolymers also yields good results, as can be seen in the study by Gholampour et al. [40], presents the behavior of geopolymers reinforced with natural fibers containing industrial by-products and waste sands, were used as fine aggregates in geopolymers reinforced with natural fibers 1 and 2% of coconut fibers, ramie, sisal, hemp, jute and bamboo, per volume fraction of fine aggregates, the results reveal that geopolymers containing 1% ramie, hemp and bamboo fiber and 2% ramie fiber exhibit higher compressive and tensile strength. According to the research of Ramakrishna and Sundararajan [41] on geopolymers reinforced with 2% sisal fibers, by weight the compressive strength value obtained at 28 days of curing was 9 MPa.

Regarding flexural strength, the study by Matalkah et al. [42] developed a geopolymers based on wheat straw ash:coal fly ash:metakaolin:gypsum in weight ratios of 0.50:0.25:0.25:0.25:0.05, providing an increase of 26% in flexural strength. Similarly, the study performed by Yang et al. [43] elaborated geopolymers with a mixed activator of sodium hydroxide, liquid sodium silicate and gypsum, yielding flexural strengths of 7.5 MPa.

It must be taken into account that geopolymers are brittle by nature, have low strength to tensile and flexural stresses and have sudden failures, but to solve this problem Mahmood et al. [44], indicates that reinforcing geopolymers with natural and synthetic fibers increases their ductility and strength to flexural stresses and that the incorporation of natural fibers in geopolymers offers a feasible solution to counteract their initial brittle behavior.

The reinforcement with natural fibers allows the material to resist tensile stress at a higher level than the geopolymer without natural fibers, so it is possible to propose a geopolymer with natural fibers that combines mechanical properties [45], as an example we can have the study conducted by Ranjithkumar et al. [46]. that the incorporation of Phoenix

sp. fibers to the geopolymer improved the tensile strength from 1.28 to 2.35 MPa.

From the review, it is clear that there are extensive studies on the use of RHA in geopolymers; whose characteristics depend on the source (composition) and how the materials are preprocessed before incorporating them into the geopolymer, such as the calcination temperature; in addition, during the manufacturing process, the setting time of the geopolymer increases with the incorporation of RHA, that is why a heat treatment prior to the RHA was performed in order to determine the optimum calcination temperature and thus have better results in the mechanical strength of the geopolymer. The knowledge gap is that only geopolymers have been manufactured with RHA where the setting time is prolonged, and they need calcium to reduce the setting time. The main objective of this study is to evaluate the geopolymer manufacturing process using the local materials; the physical, mechanical properties and microstructural characteristics of the geopolymers were studied. Parameters such as optimum calcination time of the RHA, optimum gypsum content, optimum mixing combination and optimum ichu fiber content were established. To reduce the setting time, semihydrated gypsum was used for its calcium content; furthermore, and ichu fiber was used to improve the mechanical flexural and tensile strengths of the geopolymer. In order to obtain the proper combination different proportion of sodium hydroxide, gypsum and ichu fibers were evaluated.

Materials and methods

Materials

Aggregates and water

The aggregates used were extracted from the Pátapo quarry in the Lambayeque Region—Peru, in the case of river sand with a particle size range of 4.75–75 μm with a fineness modulus of 2.93, with a nominal maximum coarse aggregate size of 19 mm according to the standards detailed in Table 1 where the physical characteristics of the aggregates are described, which will be used to determine the amount of weight per cubic meter of aggregates that will enter the geopolymer mix. The tap water used was drawn from the laboratory itself and was used for the preparation of the geopolymer and the subsequent curing sample described according to ASTM C1602 [47].

Rice husk ash (RHA)

The RHA is an agricultural bioburden or type of rice product residue from the burning of rice husk that is used as fuel, which has a particular characteristic that contains chemical

Table 1 Physical characteristics of aggregates. *Source*: Authors

| Description	Aggregates		Standard
	Fine	Coarse	ASTM
Modulus of fineness	2.93	–	C136 [48]
Loose dry unit weight (g/cm^3)	1.62	1.57	C29 [49]
Dry-rodded unit weight (g/cm^3)	1.76	1.65	
Apparent specific gravity	2.75	2.73	C128 [50]
Absorption capacity (%)	1.05	1.31	C127 [51]
Natural moisture content (%)	0.30	0.49	C566 [52]
Abrasion wear (%)	–	9.96	C131 [53]
Percentage of the finest material passing through sieve # 200	4.82	–	C117 [54]
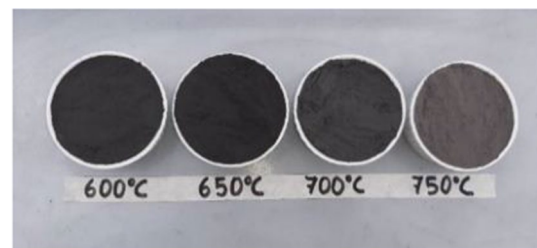
Fig. 1 RHA at 600, 650, 700 and 750 °C crushed and screened on a 325 mesh screen (45 μm). *Source*: Authors

substances with pozzolanic and cementing characteristics that if mixed with cement and water could increase strength due to its pozzolanic activity because it has main compounds such as silica and alumina, for this reason the calcination temperature must be previously analyzed to determine the highest amount of silica and alumina that it can contain [55]. In the present investigation, pozzolanic activity was determined according to ASTM C618 [56]. The RHA were calcined at 600, 650, 700 and 750 °C, grounded and sieved through mesh #325 (45 μm) as shown in Fig. 1.

Gypsum

It is the result of calcination and crushing of gypsum stone, whose hydration of the product allows the production of a mortar paste for different construction purposes. The supplementary activator semihydrated gypsum ($CaSO_4 \cdot 1/2 \cdot H_2O$) is an industrial grade reagent. For convenience, in the present investigation gypsum refers to semihydrated gypsum [57].

Ichu fiber

Stipa Obtusa is a grass plant commonly called ichu that spreads throughout the Andean region, is a shrub that is present all year round very dense, can reach 20–50 cm long,

Fig. 2 Fibra de ichu usada. *Source*: Authors

Table 2 Properties of ichu fiber

Description	Ichu fiber	Standard ASTM
Length (mm)	40 mm	–
Dimensions	0.40–2.0 mm	
Apparent specific gravity	0.26	ASTM C 188 [62]
Tensile strength	250 MPa	ASTM C 188 [63]

Fig. 3 Geopolymer production process. *Source*: [64]
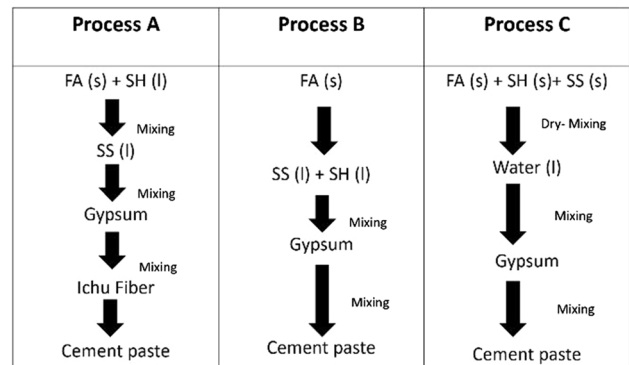
Fig. 4 Mixing processes A, B and C adopted in the present study. *Source*: Authors

with many vertical and resistant leaves, and narrow clusters of 5.0–13.0 cm and 1 to 2 mm in diameter [58]. It has been used for 50 years throughout the Andean region in the construction of roofs and as a rope material. As time went by, its use was gradually reduced. Currently, ichu treated with an alkaline solution of sodium hydroxide is being studied to characterize its properties such as crystallinity index, contact angle, thermal degradation, morphology and surface energy, showing good results [59, 60]. According to Candiotti et al. [61], they conclude that fibers obtained from Stipa Obtusa have potential and allow competition with commercial natural fibers as reinforcement in polymer matrix blends. Figure 2 shows the ichu fiber used in the present investigation. Table 2 shows the physical and mechanical characteristics of the ichu fiber used, showing an absorption of 110%, with a density of 262.70 kg/m³ and a tensile stress of 250 MPa. For the present study, ichu fibers with a length of 40 mm were used and with a rectangular cross section whose width ranged from 0.20 to 0.55 mm and height from 1.60 to 2.30 mm.

Methods

The materials used in the blend of the geopolymer studied were $RHA + NaOH + Na_2SiO_3 + CaSO_4 \cdot 1/2 \cdot H_2O + ichu$ fiber. The RHA was first verified to comply with ASTM C618 and both NaOH (SH) and Na_2SiO_3 (SS) were used as alkaline activators. The sodium silicate used in the present investigation had a ratio of silicon oxide/sodium oxide = 2.0 ($SiO_2/Na_2O = 2.0$). The SS/SH alkali mass ratio was 1.50, while the SS + SH mass ratio with respect to the RHA
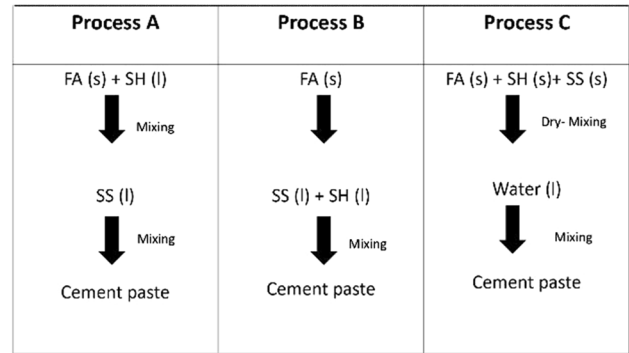
component was 0.40 for the case of the geopolymer mixture without gypsum content. Gypsum was used as a partial substitute for RHA at 10, 20, 30, 30, 40 and 50% with respect to its weight, where the SS + SH mass ratio with respect to the RHA component varied when the mixture contains gypsum by 0.44, 0.50, 0.57, 0.67 and 0.80, respectively, at 10, 20, 30, 30, 40 and 50% gypsum content. For mixing, processes A, B and C recommended by Teewara and Mitzi [64] were used, which are detailed below and can be seen in Fig. 3. According to research conducted by researcher Teewara and Mitzi, process A evidenced better mechanical strength than process B and process C evidenced the lowest mechanical strength as it solidified in less time than process A or B due to the strong hydration reaction of the primary inputs, alkaline solids and water. For the present study, the mixing processes A, B and C were adapted according to Fig. 4, gypsum was added with the purpose of accelerating the setting and improving the mechanical properties of the geopolymer made only with RHA and the addition of ichu fiber is with the objective of improving the properties of strength of the geopolymer.

In each mixing process, the molarity of sodium hydroxide was varied from 8, 10, 12 and 14 M and the amount of

coarse and fine aggregates was kept constant at 50% of the weight of the geopolymer mixture. In all cases the curing of the geopolymer was carried out at room temperature, whose specimen breaks were at 7, 14 and 28 days, and were given with the environmental characteristics as shown in Table 3.

The following steps were carried out to prepare the samples: (1) Evaluated the pozzolanic activity of RHA in a mortar cube with Portland cement in order to determine the calcination temperature, (2) the geopolymer made only with the RHA was evaluated to determine the optimum molarity, for this first stage, the mixing process used was C, (3) the geopolymer made with the rice husk ash was evaluated, with molarities 8, 10, 12 and 14 M, with the percentages of 10, 20, 30, 30, 40 and 50% gypsum in order to determine the optimum molarity and the optimum percentage of gypsum, for this second stage, the mixing process used was C, (4) with what was determined in step 2, the geopolymer was evaluated with the mixing processes A, B and C already explained above and in this way the optimum mixing process of the geopolymer was determined, and, it was found that the optimum mixing process was A (5) with what was obtained in step 4, the geopolymer was evaluated with the percentages of 0.5, 1.0, 1.5 and 2% of ichu to determine the optimum percentage of ichu, for this fourth stage, the

optimum mixing process resulting from the third stage was used. Figure 5 shows the flow diagram of the 5 steps mentioned above. For the evaluation of the geopolymer in step 1, the following treatments were carried out: T1 (8 molar-7 days); T2 (8 molar-14 days); T3 (8 molar-28 days); T4 (10 molar-7 days); T5 (10 molar-14 days); T6(10 molar-28 days); T7 (12 molar-7 days); T8 (12 molar-14 days); T9 (12 molar-28 days); T10 (14 molar-7 days); T11(14 molar-14 days); T12 (14 molar-28 days).

RHA—pozzolanic activity, unit weight and air content

Pozzolanic activity was determined using ASTM C618 [56], which consisted of testing 5 cm × 5 cm × 5 cm cubes were fabricated as a standard sample with a w/c ratio of 0.48; and then, 20% by weight of cement was replaced by the RHA at the four calcination temperatures performed in the present investigation, after which the specimens were tested for simple compressive strength under ASTM C39/C39M [66] with a loading rate of 0.25 ± 0.05 MPa/s, as shown in Fig. 6, the mixing ratios of the mortar cubes to determine the pozzolanic activity/calcination temperature are shown in Table 4. The density and air content were performed under ASTM C138/C138M [67].

Table 3 Environmental characteristics of the area where the geopolymers were cured. *Source*: Authors

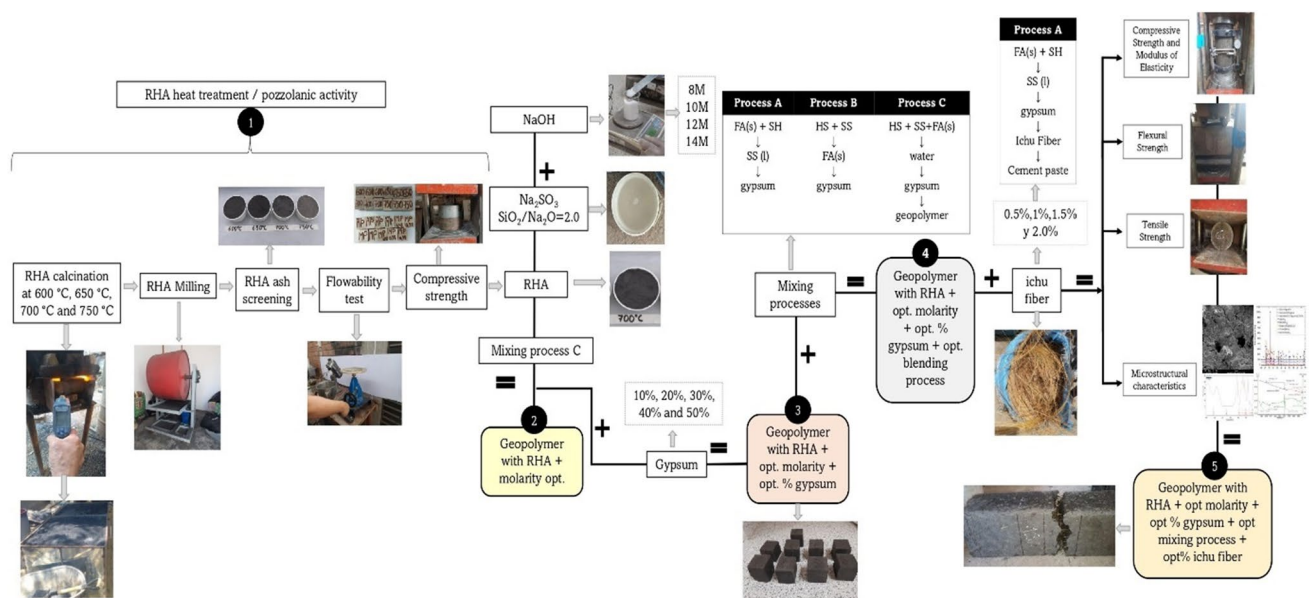| City/Country	Date	Minimum temperature (°C)	Maximum temperature (°C)	Maximum humidity (%)	Solar radiation (kWh)	Fuente
Chiclayo/Peru	12/2021–04/2022	21	31	90	6.1–6.6	[65]

Fig. 5 Processing of geopolymer samples. *Source*: Authors
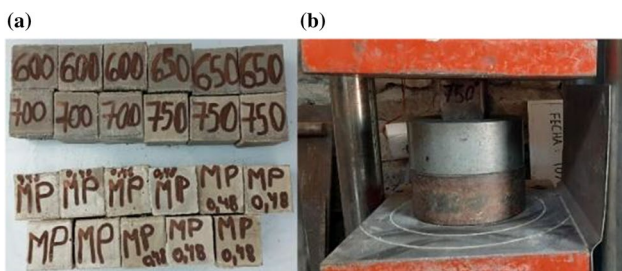
(a)   **(b)**

Fig. 6 a Specimens of 5 cm×5 cm×5 cm and **b** compressive strength test to determine the pozzolanic activity of the RHA. *Source*: Authors

Fig. 8 Cylindrical and prismatic specimens of geopolymers tested. *Source*: Authors

Compressive strength, elastic modulus, bending strength and tensile strength

The compressive strength was performed under ASTM C39/C39M [66], the calculation of the elastic modulus was carried out according to ASTM C469/C469M [68], the flexural strength was performed under ASTM C78/C78M [69], and tensile strength was performed according to ASTM C496 [70]. Figure 7 shows the mechanical strength tests performed on the geopolymers, Fig. 8 shows the cylindrical and prismatic geopolymer specimens tested.

The geopolymers were manufactured under processes A, B and C described above. The raw materials were NaOH, Na_2SiO_3, RHA calcined at 700 °C, semihydrated gypsum and natural ichu fiber, whose mixture proportions are shown in Tables 5 and 6.

For the calculation of the inputs, it was assumed that the percentage in weight per cubic meter of mixture is that the fine and coarse aggregates are 50%, so the other 50% would be occupied by the RHA, NaOH, Na_2SiO_3 and gypsum for the calculation would be as follows.

The specific gravity of the sodium hydroxide solution is 2 g/cm^3.

The specific gravity of sodium silicate is 1.45 g/cm^3.

The specific gravity of rice husk ash is 1.465 g/cm^3.

Weight of rice husk ash is = X.

Weight of sodium hydroxide = SH.

Table 4 Proportions of raw materials of the mortar used to determine the pozzolanic activity of the RHA/Optimal calcination temperature

Description	Cement (kg/m^3)	Rice husk ash (kg/m^3)	Sand (kg/m^3)	Ratio sand/cement	Water (L/m^3)
Mortar	729.68	–	973.28	1.33	350.32
Mortar + 20% of RHA (600 °C, 650 °C, 700 °C and 750 °C)	583.76	145.92	973.28	1.67	350.32

Source: Authors

Fig. 7 Mechanical strength tests **a** compression test and elastic modulus, **b** tensile strength and **c** bending test. *Source*: Authors
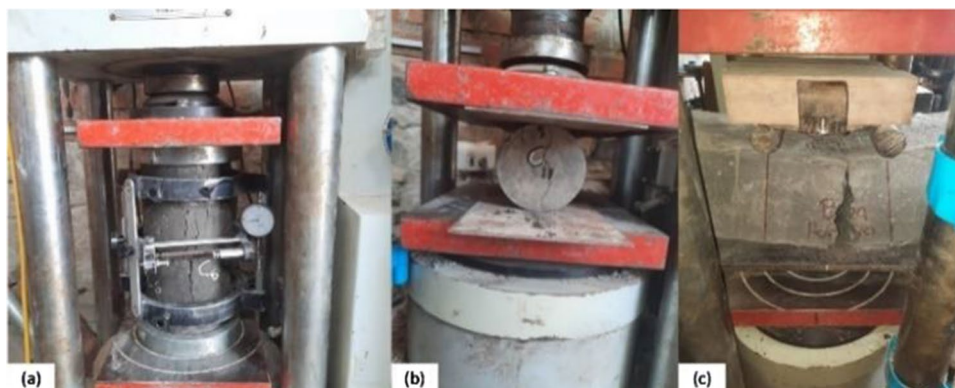
Table 5 Ratios of raw materials in the geopolymer mixture with different proportions of gypsum, NaOH and Na_2SiO_3

Molarity of sodium hydroxide + % of gypsum	Combination code	NaOH (solid) (kg/m³)	Water (kg/m³)	Sodium silicate (liquid) (kg/m³)	Gypsum (kg/m³)	RHA (kg/m³)	Sand (kg/m³)	Stone (kg/m³)
8 M + 0% gypsum	8M00G	86.2	269.5	129.3	–	539.0	665.6	358.4
8 M + 10% gypsum	8M10G	86.2	269.5	129.3	53.9	485.1	665.6	358.4
8 M + 20% gypsum	8M20G	86.2	269.5	129.3	107.8	431.2	665.6	358.4
8 M + 30% gypsum	8M30G	86.2	269.5	129.3	161.7	377.3	665.6	358.4
8 M + 40% gypsum	8M40G	86.2	269.5	129.3	215.6	323.4	665.6	358.4
8 M + 50% gypsum	8M50G	86.2	269.5	129.3	269.5	269.5	665.6	358.4
10 M + 0% gypsum	10M00G	92.2	230.4	138.3	–	576.1	674.05	362.95
10 M + 10% gypsum	10M10G	92.2	230.4	138.3	57.6	518.5	674.05	362.95
10 M + 20% gypsum	10M20G	92.2	230.4	138.3	115.2	460.9	674.05	362.95
10 M + 30% gypsum	10M30G	92.2	230.4	138.3	172.8	403.3	674.05	362.95
10 M + 40% gypsum	10M40G	92.2	230.4	138.3	230.4	345.7	674.05	362.95
10 M + 50% gypsum	10M50G	92.2	230.4	138.3	288.1	288.1	674.05	362.95
12 M + 0% gypsum	12M00G	93.7	195.2	140.5		585.6	659.75	355.25
12 M + 10% gypsum	12M10G	93.7	195.2	140.5	58.6	527.0	659.75	355.25
12 M + 20% gypsum	12M20G	93.7	195.2	140.5	117.1	468.5	659.75	355.25
12 M + 30% gypsum	12M30G	93.7	195.2	140.5	175.7	409.9	659.75	355.25
12 M + 40% gypsum	12M40G	93.7	195.2	140.5	234.2	351.3	659.75	355.25
12 M + 50% gypsum	12M50G	93.7	195.2	140.5	292.8	292.8	659.75	355.25
14 M + 0% gypsum	14M00G	89.7	160.2	134.5		560.6	614.25	330.75
14 M + 10% gypsum	14M10G	89.7	160.2	134.5	56.1	504.5	614.25	330.75
14 M + 20% gypsum	14M20G	89.7	160.2	134.5	112.1	448.5	614.25	330.75
14 M + 30% gypsum	14M30G	89.7	160.2	134.5	168.2	392.4	614.25	330.75
14 M + 40% gypsum	14M40G	89.7	160.2	134.5	224.2	336.4	614.25	330.75
14 M + 50% gypsum	14M50G	89.7	160.2	134.5	280.3	280.3	614.25	330.75

Source: Authors

Table 6 Proportions of raw materials in the geopolymer mixture with the optimum content of gypsum, NaOH and Na_2SiO_3 and different proportions of ichu fiber. *Source*: Authors

Optimum molarity of sodium hydroxide + optimum % of gypsum + % of ichu fiber	Combination code	NaOH (kg/m³)	Water (kg/m³)	Silicate (kg/m³)	Gypsum (kg/m³)	RHA (kg/m³)	Sand (kg/m³)	Stone (kg/m³)	Ichu fiber (kg/m³)
12 M + 20% gypsum + 0.5% natural ichu fiber	12M20G0.5IF	93.7	195.2	140.5	117.1	468.5	659.75	355.25	10.15
12 M + 20% gypsum + 1.0% natural ichu fiber	12M20G1.0IF	93.7	195.2	140.5	117.1	468.5	659.75	355.25	20.3
12 M + 20% gypsum + 1.5% natural ichu fiber	12M20G1.5IF	93.7	195.2	140.5	117.1	468.5	659.75	355.25	30.45
12 M + 20% gypsum + 2.0% natural ichu fiber	12M20G2.0IF	93.7	195.2	140.5	117.1	468.5	659.75	355.25	40.6

Weight of sodium silicate = SS

$$\frac{SH + SS}{X} = 0.40, \quad X = 6.25SH$$

$$\frac{X}{1450 \text{ kg/m}^3} + \frac{SH}{2000 \text{ kg/m}^3} + \frac{SS}{1450 \text{ kg/m}^3} = 0.50 \text{ m}^3$$

$$\frac{X}{1450 \text{ kg/m}^3} + \frac{SH}{2000 \text{ kg/m}^3} + \frac{1.5SH}{1450 \text{ kg/m}^3} = 0.50 \text{ m}^3$$

$$0.00068X + 0.0015SH = 0.5 \text{ kg}$$

$$0.0043SH + 0.0015SH = 0.5 \text{ kg}$$

$$0.0058SH = 0.5 \text{ kg}$$

$$SH = 86.2 \text{ kg}$$

$$SS = 1.5 \times 86.2 \text{ kg} = 129.3 \text{ kg}$$

$$RHA = \frac{86.2 + 129.3}{0.40} = 538.8 \text{ kg}$$

This calculation is repeated for all the mixing sequences listed in Tables 5 and 6.

Microstructural characteristics

Fourier transform infrared (FTIR) spectroscopy It was carried out under ASTM E1252-21 standard [71], to analyze the chemical structure of the hardened pastes. A Tensor 27 FTIR Infrared Spectrometer with KBr pellet was used. The sample was ground, sieved through a 100 mesh sieve and mixed with KBr in a 20:1 ratio (KBr:Geopolymer), treated according to ASTM E1252-21.

Thermogravimetric analysis (TGA) The experiments were performed under ASTM E1131-20 [72], the experiments were carried out with a thermogravimetric analyzer STA 449F3, with a temperature range of 30–990 °C at a rate of 10 °C/min, purge gas: Nitrogen 30 to 600 °C/Oxygen 600 to 990 °C and with a gas flow rate of 50 ml/min.

Scanning electron microscopy (SEM) and EDS characterization The measurements were carried out with a scanning electron microscope (SEM) of FEI model Quanta 200, for which an accelerating voltage of 30 kV and a spot size of 6 were used, both for the images and for the composition.

Areas were measured at 200×, 400× and 500× magnifications, depending on the features to be imaged. Energy dispersive X-ray spectroscopy (EDS) measurements were performed with an EDAX detector mounted on the electron microscope. Data processing and elemental composition determination was performed with EDAX Genesis XM 4 software, using a ZAF matrix correction. Regarding sample preparation, fragments with features of interest were selected and mounted on aluminum posts for electron microscopy with carbon adhesive tape and fixed with copper tape. All samples were coated with a thin layer of 20–40 nm of gold, in order to make their surface conductive and facilitate high vacuum imaging. The presence of gold was deliberately excluded from the EDS compositional analysis.

X-ray diffraction (XRD) X-ray diffraction analysis was performed with Bruker XRD equipment model D8 Discover with copper radiation ($Cu_{K\alpha} = 0.15418$ nm), 40 mA current and 40 kV accelerating voltage, with a Lynxeye detector with energy selectivity. The diffractogram was obtained in a range of angles (2θ) from 5 to 80 degrees in steps of 0.02 degrees. The time per step was 1 s. To calculate the composition of the crystalline phases and the amorphous part, the Reference Intensity Ratio method was applied. The minimum concentration for this method is 0.1 wt%.

Results and discussion

RHA—pozzolanic activity—portland cement mortar

The determination of the pozzolanic activity of the RHA was carried out according to ASTM C618, Fig. 9 shows the results of the pozzolanic activity of rice husk ash.
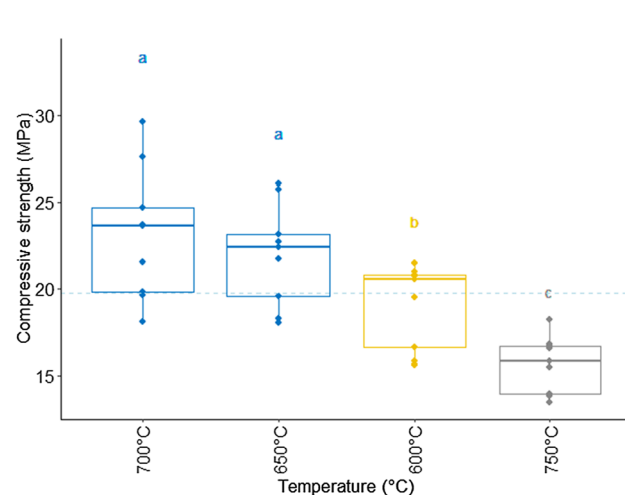
Considering the results of Fig. 9, the application of the two-factor transformed aligned ranks showed that the interaction of the factors did not present a significant effect (p value $= 0.054862 > 0.05$) on the compressive strength, but a significant effect was evidenced in the main factors, both in the temperature factor (p value $= 2.4721e-10 < 0.05$), and in the curing days factor (p value $= 2.0893e-07 < 0.05$).

The best combination, according to Tukey's multiple comparison post hoc test, the 700 °C temperature level and 28 days of curing, the levels that allowed maximizing the compressive strength because they were the levels that presented the highest averages (23.14 MPa, for the 700 °C level and 21.99 MPa, figure reached at 28 days of curing), and the best combination, according to Tukey's multiple comparison post hoc test, was the level of temperature 700 °C and 28 days of curing.

Table 7 shows the quantities of the chemical compounds contained in the RHA and the method of analysis used to obtain them, showing that the amount of silica is 71.50% and alumina is 0.38%, varying significantly the silica content

Table 7 Chemical analysis of the RHA (%). *Source*: Authors

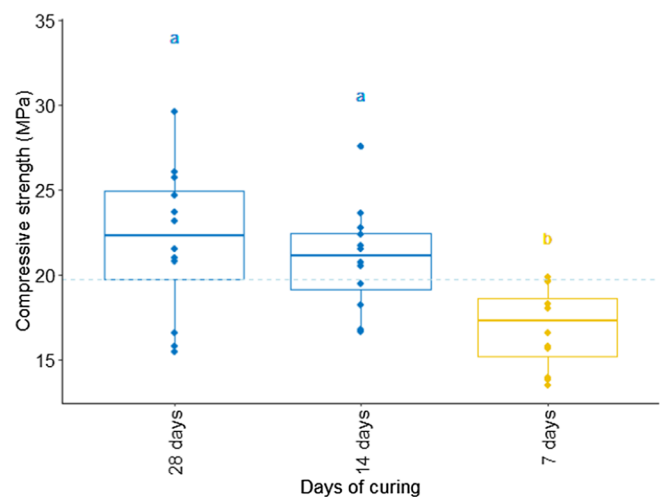| Chemical composition	Method of analysis	Result (%)
SiO_2	Gravimetric	71.50
Al_2O_3	Atomic absorption	0.38
FeO	Atomic absorption	0.45
CaO	Atomic absorption	0.88
Na_2O	Atomic absorption	0.38
TiO_2	Atomic absorption	< 0.01
MgO	Atomic absorption	0.36
K_2O	Atomic absorption	2.43
SO_3	ICP OES	0.25

Fig. 9 Variation of compressive strength of Portland cement mortar as a function of RHA calcination temperature and days of curing. *Source*: Authors

by 15.26% compared to the results obtained by Abd-Ali and Kadhim [21], this explanation could be given because the optimum calcination temperatures are between 500 and 600 °C, while in the present investigation the optimum calcination temperature is 700 °C. According to the chemical requirements of the ASTM C618, the RHA used is of class F.

Unit weight and air content

The density varied from 1.89 to 2.074 g/cm^3, observing that the density increases until reaching 10 M and decreases each time the molarity of sodium hydroxide is increased, these results are similar with the research of Öztürk that manifests that 12 M geopolymers, have an average unit weight of 1.535 g/cm^3 and 1.692 g/cm^3 with a SS/SH ratio of 2 and 2.5 [23], and are also close to those obtained by researchers [24, 25]. For the case of air content varies from 1.8 to 3%, increasing each time the molarity of sodium hydroxide increases, this result agrees with the investigations of Kotop et al. and Saloni et al. [27, 28]. The results of unit weights and air content according to molarity can be seen in Figs. 10 and 11, respectively.

Compressive strength and elastic modulus

Figure 12 shows the treatments are: T1 (8 molar-7 days); T2 (8 molar-14 days); T3 (8 molar-28 days); T4 (10 molar-7 days); T5 (10 molar-14 days); T6 (10 molar-28 days); T7 (12 molar-7 days); T8 (12 molar-14 days); T9 (12 molar-28 days); T10 (14 molar-7 days); T11 (14 molar-14 days); T12 (14 molar-28 days), reaching a compressive strength of 2.34 MPa. The results obtained are similar to those obtained by Ilmiah whose compressive strength was 2.58 MPa [36] and very close to the results performed by researchers Somna et al. [13], where RHA was used to replace FA up to 50%, obtaining a compressive strength
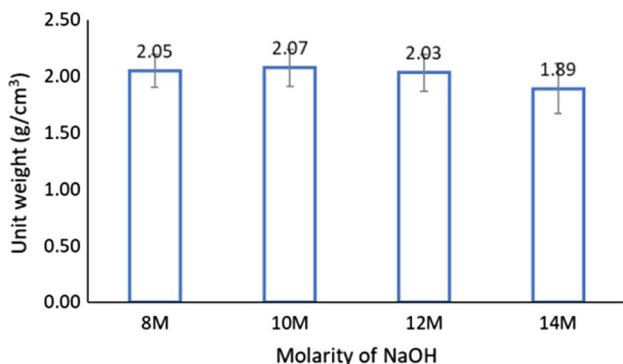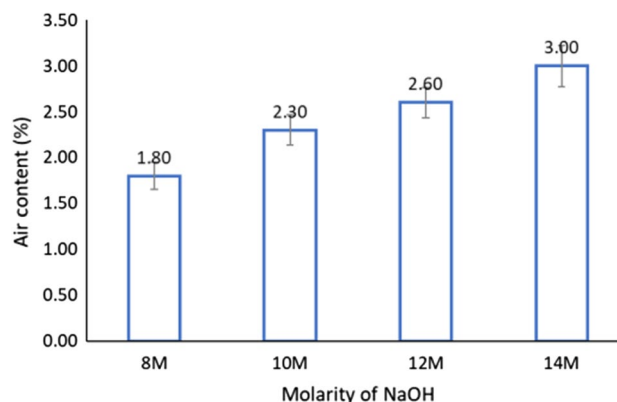

Fig. 11 Variation of geopolymer air content as a function of sodium hydroxide molarity ratios. *Source*: Authors

of 4.1 MPa, which contrasts with the results obtained by Lianasari et al. [29], who elaborated geopolymers based on FA:RHA in proportions of 40:60, whose result was 4.08 MPa, respectively. Lower alkalinity negatively affects the mechanical properties of the cements because the ionic strength generated in the activator-agglutinant system is not high enough to hydrolyze satisfactorily the silicon and aluminum present in the starting material [73] (Fig. 12).

Figure 13 shows that the treatment of 12 Molar×20% gypsum×28 days of cure (12M20G), reaching a maximum compressive strength of 8.01 MPa, was the most effective treatment for the treatment of the 12 Molar×20% gypsum×28 days of cure (12M20G). These results can be compared with the research of Januar et al. [33] whose results showed that geopolymers made at 12 M NaOH obtained compressive strength of 9.87 MPa and the results of An et al. [38] reveal that geopolymers with a dose of 5% gypsum was beneficial to increase the value of compressive strength to 9.31 MPa, and these results are very similar to those found in the present investigation. The results of the present investigation agree with the results of Handayani et al. [34], indicating that increasing the molarity of sodium hydroxide does not necessarily increase the mechanical strength of the geopolymer. The increase in mechanical strength is due to the presence of calcium in the gypsum, which accelerated the dissolution of the RHA generating alkali metal cation supply [73].

According to the results of Fig. 14 shows the mechanical strengths with the optimal molarity (12 Molar), optimal percentage of gypsum (20% gypsum), with the mixing processes A, B and C broken at 7, 14 and 28 days of curing, it was evidenced that the best treatment was the mixture A×28 days of curing, reaching an average strength of 9.72 MPa, while in the elastic modulus variable, the best treatment was the mixture A at 28 days, reaching an average of 5917.79 MPa.

Fig. 10 Variation of geopolymer unit weight as a function of sodium hydroxide molarity ratios. *Source*: Authors

Fig. 12 Compressive strength (MPa) of the geopolymer by treatment, according to the combination of molar factor levels and days of cure. *Source*: Authors
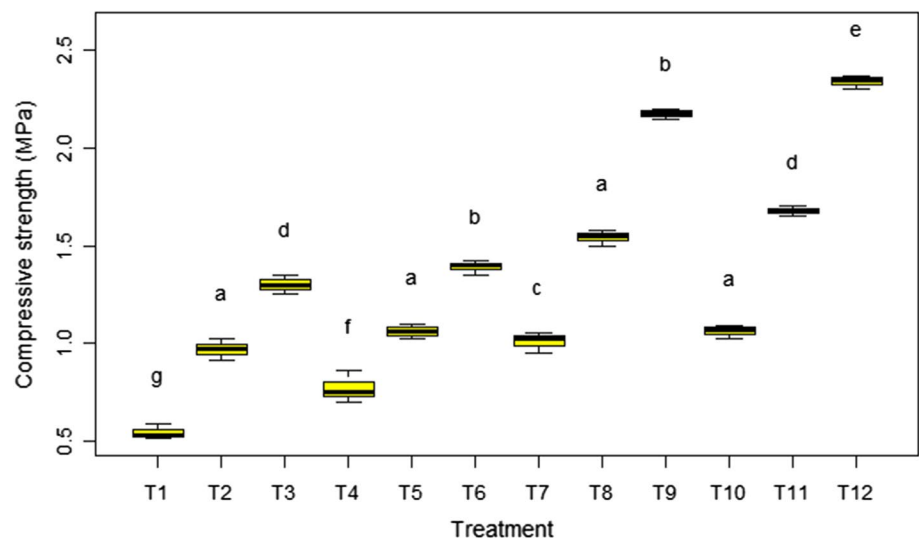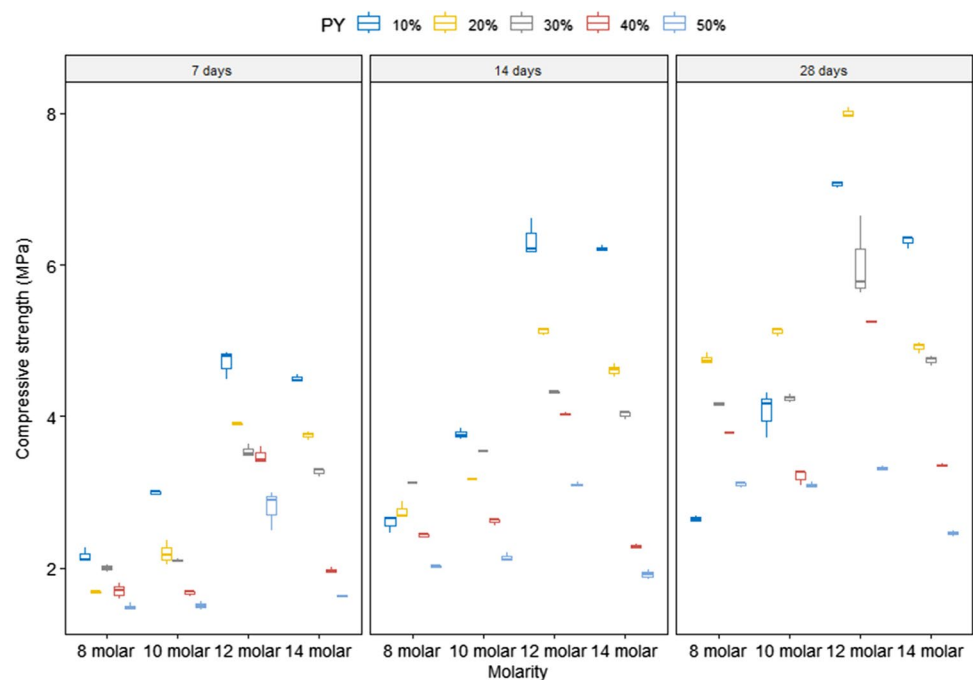

Fig. 13 Compressive strength (MPa) of geopolymer by treatment, according to the combination of molar factor levels, percentage of gypsum and days of cure. *Source*: Authors

It was verified that the setting time significantly influences the evolution of the compressive strength and the elastic modulus, the mixing process A than processes B and C. This result agrees with researchers Teewara and Mitzi [64] indicating that process A resulted in higher mechanical strength than process B and C.

According to the results in Fig. 15, the mechanical strengths are shown with the optimal molarity (12 molar), optimal percentage of gypsum (20% gypsum), with the optimal mixture and with percentages of 0.5, 1, 1.5 and 2% of broken ichu fiber at 7, 14 and 28 days of curing, showing that the best was 1.5% of ichu fiber × 28 days of curing with

a compressive strength of 12.52 MPa and an elastic modulus of 7385.02 MPa.

These results are similar to those found by Ramakrishna and Sundararajan [41] in geopolymers reinforced with sisal fibers in 2%, in weight with a compressive strength that 9 MPa, similarly, the study conducted by Gholampour et al. [40] presents the characteristics of geopolymers reinforced with natural fibers containing waste sands and industrial by-products reinforced with vegetable fibers of 1 and 2% of coconut, jute, ramie sisal, hemp and bamboo fibers, per volume fraction of fine aggregates, presenting a higher compressive strength.
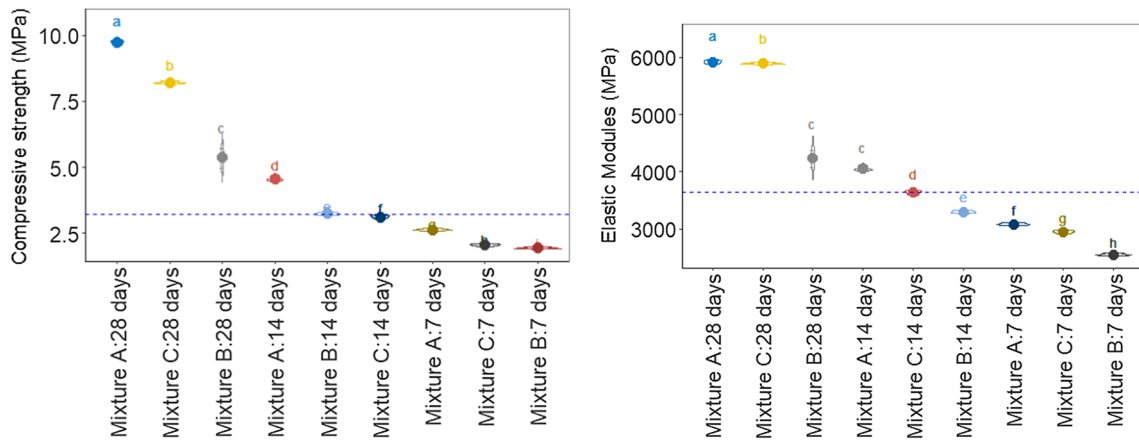
Fig. 14 Compressive strength and elastic modulus of geopolymer 12M20G, with mix processes A, B and C broken at 7, 14 and 28 days of cure. *Source*: Authors
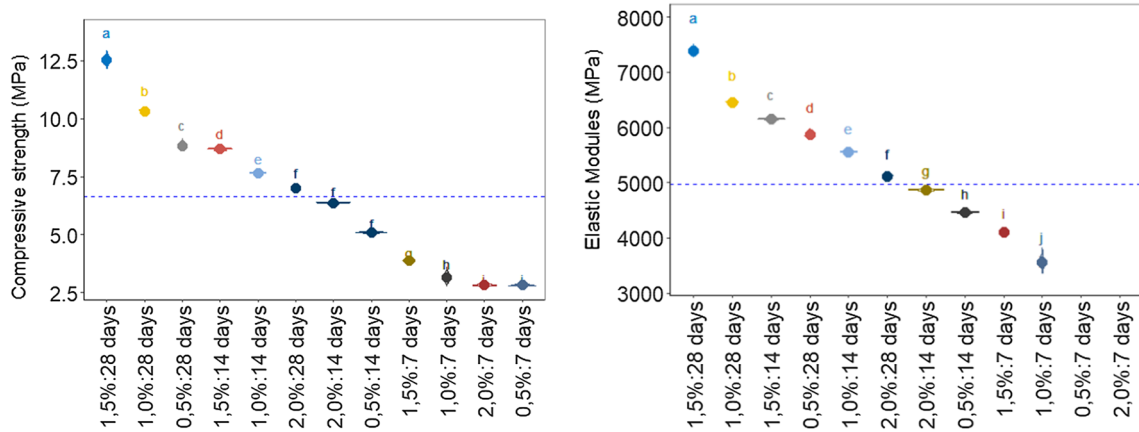

Fig. 15 Compressive strength and elastic modulus of geopolymer 12M20G, with the optimum blend a0nd with 0.5, 1, 1.5 and 2% ichu fiber, broken at 7, 14 and 28 days of cure. *Source*: Authors

Bending strength

Figure 16 shows the flexural strength with the optimum molarity (12 molar), optimum percentage of gypsum (20% gypsum), with the mixing processes A, B and C broken at 7, 14 and 28 days of curing, it was evidenced that the treatment that presented the highest average flexural strength was the one obtained with mix C at 28 days, reaching an average value of 3.24 MPa.

Figure 17 shows the flexural strength with the optimum molarity (12 molar), optimum percentage of gypsum (20% gypsum), with the optimum mix and with a percentage of 0.5, 1, 1.5 and 2% of broken ichu fiber at 7, 14 and 28 days of curing, showing that the best treatment is the treatment of 1.5% ichu fiber at 28 days of curing.

The average obtained with the optimal treatment was 7.99 MPa in the flexural strength variable, as can be observed in the results there is an improvement in the flexural strength of geopolymers with the addition of ichu fibers, this is due to the contribution of resistance offered by the ichu fiber, since according to their results the tensile strength of the ichu fiber used is 250 MPa, this tensile strength increases the flexural strength of the geopolymer, this is due to the contribution of resistance offered by the ichu fiber, since according to their results the tensile strength of the ichu fiber is 250 MPa, this tensile strength increases the flexural strength of the geopolymer, this improvement is noted in the study conducted by Mahmood et al. [44] and with the research of Matalkah et al. [42] it can be proved that geopolymers made from wheat straw ash:coal fly ash:metakaolin:gypsum in weight ratios of 0.50:0.25:0.25:0.25:0.05 provide 26% increase in flexural strength another similar study was conducted by Yang et al. [43] where they made geopolymers with a
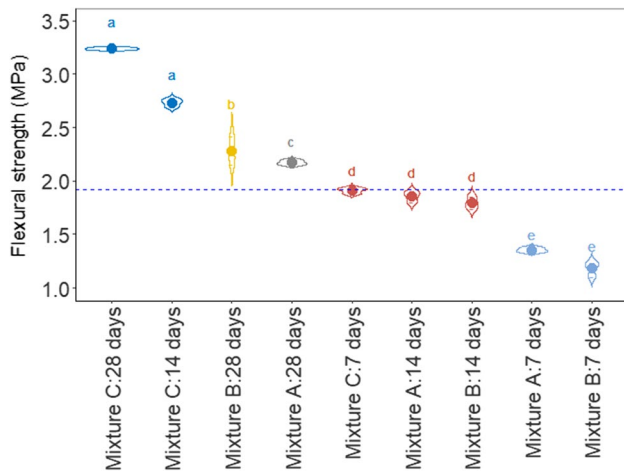
Fig. 16 Flexural strength with geopolymer 12M20G, with mix processes A, B and C broken at 7, 14 and 28 days of cure. *Source*: Authors
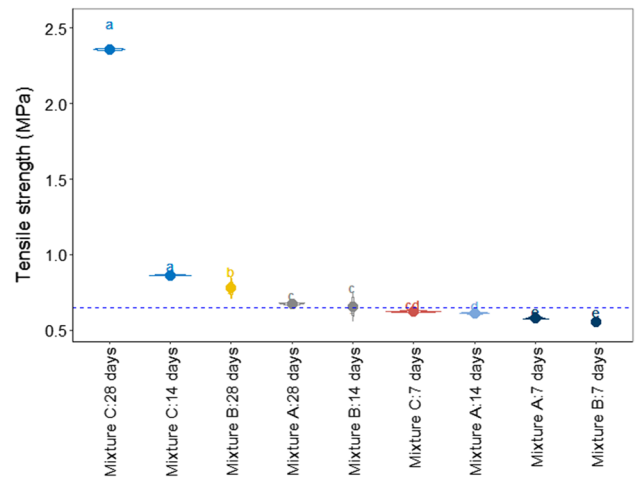

Fig. 18 Tensile strength with the geopolymer 12M20G, with mixing processes A, B and C broken at 7, 14 and 28 days of cure. *Source*: Authors
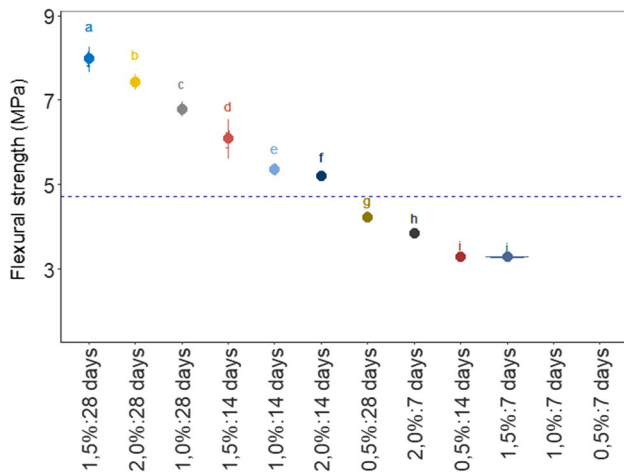

Fig. 17 Flexural strength with geopolymer 12M20G, with optimum mixing and with 0.5, 1, 1.5 and 2% percentage of broken ichu fiber at 7, 14 and 28 days of curing. *Source*: Authors
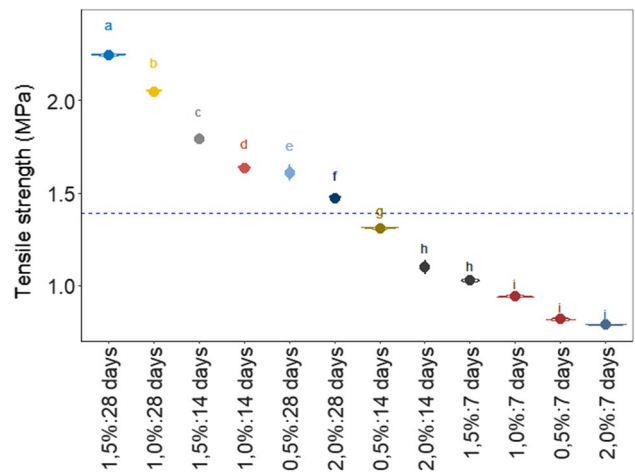

Fig. 19 Tensile strength with geopolymer 12M20G, at optimum mixing and with 0.5, 1, 1.5 and 2% broken ichu fiber at 7, 14 and 28 days of curing. *Source*: Authors

mixed activator of sodium hydroxide, liquid sodium silicate and gypsum, yielding flexural strengths of 7.5 MPa.

Tensile strength

Figure 18 shows the tensile strength with the optimum molarity (12 molar), optimum percentage of gypsum (20% gypsum), with mix processes A, B and C broken at 7, 14 and 28 days of curing, it was evidenced that the treatment that presented the highest average tensile strength was the one obtained with mix C at 28 days, reaching an average value of 2.36 MPa.

Figure 19 shows the tensile strength with the optimum molarity (12 molar), the optimum percentage of gypsum (20% gypsum), with the optimum mixture and with a percentage of 0.5, 1, 1.5 and 2% of broken ichu fiber at 7, 14 and 28 days of curing, showing that the best treatment is the treatment of 1.5% ichu fiber at 28 days of curing, reaching a tensile strength of 2.25 MPa.

In the present study, the addition of ichu fiber did not improve the tensile strength as other natural fibers have done in other studies such as that of Correia et al. [45] indicating that the reinforcement with natural fibers allows the material to resist tensile strength at a higher level than the geopolymer without natural fibers, but the

result of the present investigation is similar to the result obtained by Ranjithkumar et al. [46] where the incorporation of Phoenix sp. fibers to the geopolymer improved the tensile strengths from 1.28 to 2.35 MPa.

X-ray diffraction (XRD)

XRD: gypsum and RHA

Figure 20 shows the mineral compositions of the gypsum solid activators to be used. The gypsum used was obtained from the dehydration of $CaSO_4 \cdot 1/2 \cdot H_2O$ from quarries located in the city of Morrope in the Lambayeque Region [57]. Figure 4 shows the XRD test results of the semihydrated gypsum ($CaSO_4 \cdot 1/2 \cdot H_2O$) used in the present study. The X-ray diffraction analysis was performed DRX Bruker model D8-Focus, a Cu tube was used whose wavelength, corresponding to Kα1-Cu, is λ = 1.5406 Å. The diffractogram was obtained in a range of angles (2Θ) from 5 to 100 degrees in steps of 0.02°, with time per step was 0.5 s, and tube output voltage of 40 kV, tube output current of 40 mA, with a Lynxeye PSD detector.

Figure 21 shows the X-Ray Diffraction of the RHA, showing the concentration of 20.7% Cristobalite, 7.7% Quartz and 71.6% amorphous crystalline phase.
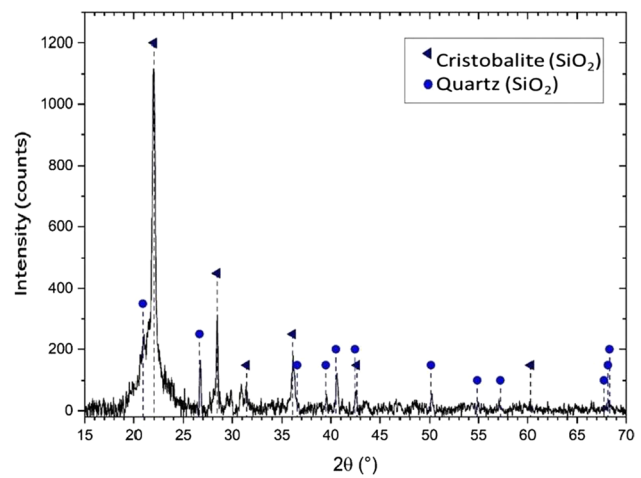

Fig. 21 X-ray diffractogram of the RHA sample and the crystalline phases identified. *Source*: Authors

XRD: geopolymer

Figure 22 shows the XRD analysis of the geopolymer pulverized past the #100 mesh with the optimum molarity (12 Molar), optimum percentage of gypsum (20% gypsum), with the optimum mixed and at 1.5% of ichu fiber. The main mineral ingredients of the geopolymer can be seen in Table 8 where quartz varies between 13.5 and 25.2%, albite between 14.5 and 15.9%, alunogen between 10 and 15.1%,
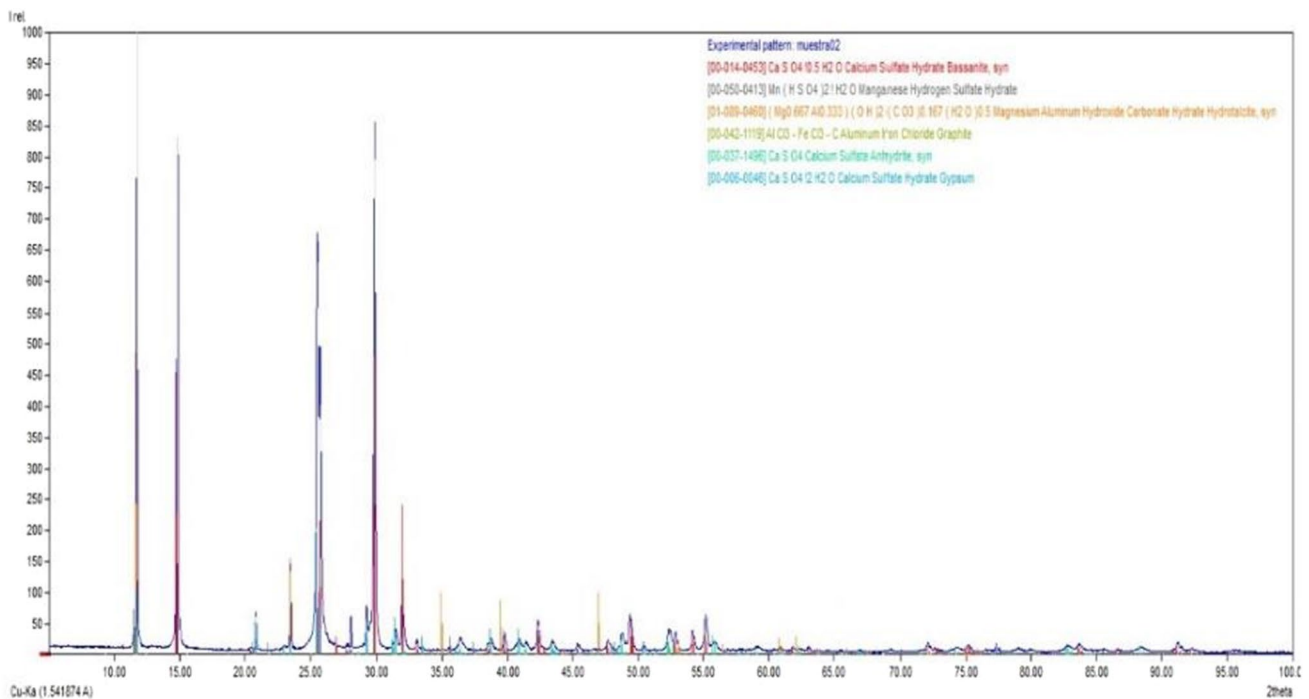

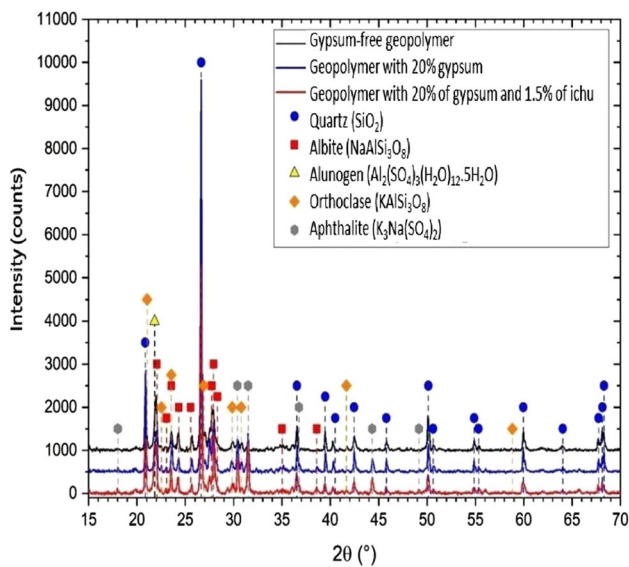**Fig. 20** XRD analysis of semihydrated gypsum ($CaSO_4 \cdot 1/2 \cdot H_2O$). *Source*: Authors

Fig. 22 X-ray diffractograms of the "Geopolymers" samples and crystalline phases identified. *Source*: Authors

the geopolymer shows a diffuse halo with 2 h values between 20 and 57, which is a typical characteristic of geopolymer gels [74].

Scanning electron microscopy (SEM) and EDS characterization

To maximize the information that can be seen visually in the SEM images, we have chosen to show combined images. These superimpose the signals from the backscattered electron detector with that from the secondary electron detector in a single image. This allows both morphological (secondary) and compositional (backscattered) features to be seen. Each sample is presented below.

M1: geopolymer pieces without gypsum

Figure 23 shows a 200× image, where various features that have been pointed out can be observed. The presence of cracking can be seen around the entire measured area, as well as some porosity in the shape of the two holes
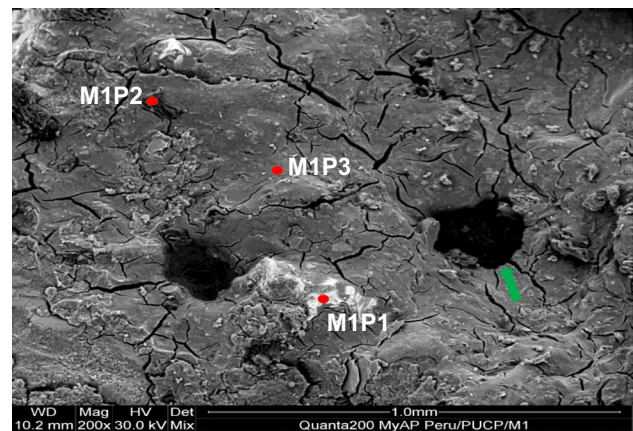
orthoclase between 6.1 and 7.7%, aphthalite between 5.1 and 5.5% and the amorphous crystalline phase between 35.6 and 46.4%. These results are similar to those of the researchers Chao-Lung and Trong-Phuoc and Handayani et al. [31, 34]. The XRD pattern of the geopolymer in Fig. 22 shows a broad peak indicating that most of the geopolymer structure and a number of non-dissolvable ingredients in the RHA such as quartz persisted, however, these peaks reduced in intensity, showing that the family materials were not fully dissolved in the inorganic polymeric materials. The differences in crystalline intensities had a clear impact on the compressive stresses of the geopolymers. The strength achieved decreased as the intensity of the crystalline phases decreases. This phenomenon corresponds with the results of the compressive strength tests mentioned above [74]. On the other hand, the presence of minor crystalline phases in the geopolymer samples such as orthoclase and aphthalite is one of the most important findings in the data collected in this research by XRD analysis [75]. The XRD diffractogram of

Fig. 23 Micrograph of sample M1—"Geopolymer chunks without gypsum" at 200× with regions of interest highlighted. *Source*: Authors

Table 8 Concentration of crystalline phases in the sample "Geopolymer without gypsum," "Geopolymer with 20% gypsum" and "Geopolymer with 20% gypsum z 1.5% ichu"

Crystalline phase	Geopolymer 12 M without gypsum (wt%)	Geopolymer 12M20G (wt%)	Geopolymer 12M20G1.5IF (wt%)
Quartz (SiO_2)	17.7	25.2	13.5
Albite ($NaAlSi_3O_8$)	15.9	15.9	14.5
Alunogen ($Al_2(SO_4)_3(H_2O)_{12} \cdot 5H_2O$)	15.1	10.0	14.5
Orthoclase ($KAlSi_3O_8$)	7.6	7.7	6.1
Aphthalite ($K_3Na(SO_4)_2$)	–	5.5	5.1
Amorphous	43.5	35.6	46.4

Table 9 Chemical composition measured by EDS in various regions of interest of sample M1—"Geopolymer chunks without gypsum"

Chemical element	Total area		M1P1		M1P2		M1P3	
	wt%	at%	wt%	at%	wt%	at%	wt%	at%
C	–	–	–	–	67.04	76.74	–	–
O	45.74	60.21	46.39	60.75	18.24	15.68	44.96	59.49
Na	8.05	7.37	8.20	7.48	6.52	3.90	7.62	7.02
Al	3.04	2.38	2.04	1.58	–	–	4.07	3.19
Si	34.01	25.50	34.41	25.67	5.65	2.77	34.02	25.64
Cl	–	–	–	–	0.43	0.17	–	–
K	6.77	3.64	7.23	3.87	2.11	0.74	6.89	3.73
Fe	2.39	0.90	1.74	0.65	–	–	2.46	0.93
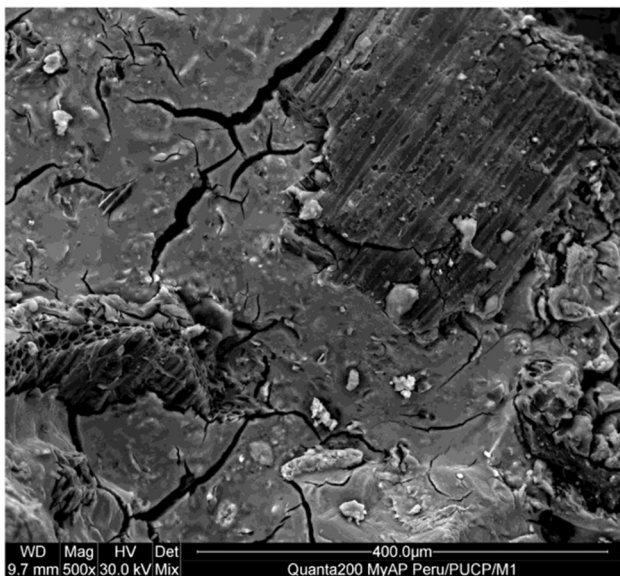
Fig. 24 Micrograph of sample M1—"Geopolymer chunks without plaster" at 500x. *Source*: Authors

Fig. 25 Micrograph of sample M2—"Chunks of geopolymers with 20% gypsum" at 200× with regions of interest highlighted. *Source*: Authors

M2: "Geopolymer chunks with 20% gypsum"

Figure 25 shows a 200× image, where regions of interest have again been marked. Three well differentiated regions can be seen, and it can be appreciated that the parts labeled M2P1 and M2P2 correspond to inclusions of different materials. The region labeled M2P3 appears to be representative of the bulk of the sample, with more pronounced cracking than the previous sample. The latter is consistent with the visual appearance of the sample, which is considerably less rigid and more granular than the previous one. In Table 10 we show the elemental compositions by EDS in the regions of interest, as well as of the entire image area, showing the major elements. The composition of the total area, as well as the M2P3 region, is similar to the previous sample. At the same time, the presence of sodium, potassium and sulfur is observed, which are consistent with the presence of gypsum in the sample. The M2P2 region, in contrast, appears to be a mineral inclusion of silicon oxide, possibly quartz (SiO_2). However, atomic concentrations suggest that its composition appears to be silicon monoxide (SiO). Unactivated silica particles are shown throughout the geopolymer matrix

marked with green arrows. There are also what appear to be inclusions of other materials, for example, in the regions labeled M1P1 and M1P2. The region labeled M1P3 corresponds to the predominant material throughout the image. In Table 9 we show the elemental compositions by EDS in the regions of interest, as well as of the whole image area, showing the majority elements. It can be seen that despite the apparent contrast with the surroundings, the M1P1 region has a composition very similar to that of the sample in general, as well as that of the M1P3 region. The origin of this contrast may be due to loading effects in the sample. The M1P2 region, in contrast, contains a high concentration of carbon, as well as a measurable presence of chlorine. This, in conjunction with its fibrous appearance, may be indicative of an ash fragment of plant origin. Figure 24 shows magnified regions at 500×, where the morphology of the sample and the presence of the high-carbon inclusions can be better appreciated.
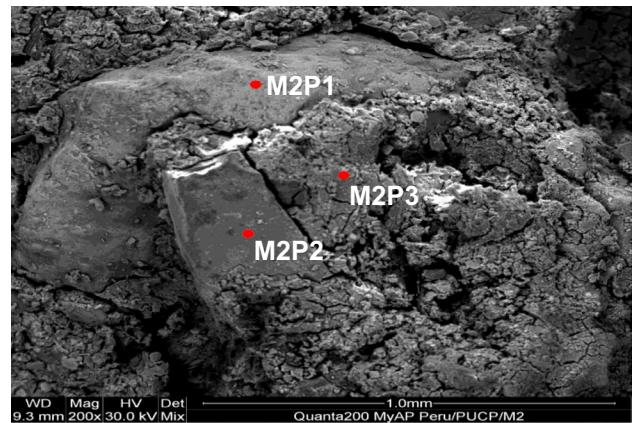
Table 10 Chemical composition measured by EDS in various regions of interest of sample M2—"Geopolymer chunks with 20% gypsum" (Fig. 25). *Source*: Authors

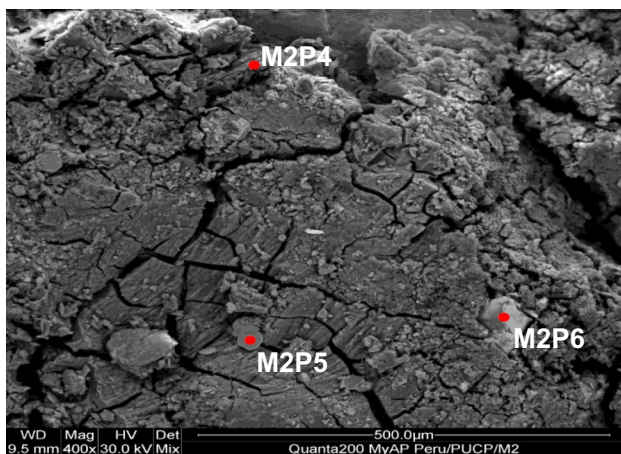| Chemical element	Total area		M2P1		M2P2		M2P3	
	wt%	at%	wt%	at%	wt%	at%	wt%	at%
O	45.07	60.20	39.66	58.87	36.26	49.97	45.97	60.17
Na	7.39	6.87	1.65	1.71	–	–	10.22	9.31
Al	2.43	1.93	5.36	4.72	–	–	1.84	1.42
Si	30.33	23.08	20.54	17.37	63.74	50.03	31.07	23.17
S	2.50	1.67	–	–	–	–	2.03	1.33
K	6.14	3.36	0.64	0.39	–	–	6.08	3.26
Ca	3.70	1.97	19.33	11.45	–	–	2.03	1.06
Ti	–	–	0.56	0.28	–	–	–	–
V	–	–	0.04	0.02	–	–	–	–
Mn	–	–	0.23	0.10	–	–	–	–
Fe	2.44	0.93	11.98	5.09	–	–	0.75	0.28

Fig. 26 Micrograph of sample M2—"Geopolymer chunks with 20% gypsum" at 400× with regions of interest highlighted. *Source*: Authors

influencing the results obtained from the mechanical tests of the geopolymer, since the unreacted material is unlikely to resist, possibly the evidence of unactivated material is due to the excess of silicon ions in the geopolymer matrix, since the evidence of this material is produced with 5 and even up to 24 days of curing [76]. Figure 26 shows a 400× image of another region of the same sample, where more regions of interest have been noted. The same carbon-rich inclusions from the previous sample can be seen in the M2P4 region, as well as other material in the M2P5 and M2P6 regions. The elemental compositions in these regions are shown in Table 11. It is verified that the M2P4 region contains a high concentration of carbon. The M2P5 region appears to be a gypsum crystal or fragment, given its high sulfur concentration, although there is a notable absence of calcium. The M2P6 region appears to be a mineral inclusion of another type, given the presence of zirconium. This material was not observed in the XRD measurements, suggesting its presence in the sample is of low concentration.

Table 11 Chemical composition measured by EDS in various regions of interest of sample M2—"Geopolymer chunks with 20% gypsum" (Fig. 26). *Source*: Authors

Chemical element	M2P4		M2P5		M2P6	
	wt%	at%	wt%	at%	wt%	at%
C	75.17	83.00	–	–	–	–
O	14.68	12.17	32.71	50.64	13.40	42.94
Na	3.25	1.87	8.55	9.21	0.83	1.85
Al	–	–	–	–	0.30	0.57
Si	4.37	2.07	–	–	4.28	7.81
S	0.43	0.18	21.08	16.29	–	–
Cl	0.17	0.06	–	–	–	–
K	1.54	0.52	37.66	23.86	0.92	1.21
Ca	0.39	0.13	–	–	0.41	0.52
Fe	–	–	–	–	0.59	0.54
Zr	–	–	–	–	79.28	44.56

M3: "Geopolymer chunks with 20% gypsum + 1.5% ichu"

Figure 27 shows a 500× image with several points of interest highlighted. As can be seen in the image, this sample is quite heterogeneous and contains fibers and other features that are of plant origin, as can be seen in regions M3P1 and M3P3. The presence of the same high carbon content inclusions is observed, for example in the M3P5 region, as well as the base material in the M3P2 region. Table 12 shows the elemental composition of these regions. Geopolymer sample obtained by EDS, the presence of oxygen, carbon and silicon is noted, so the SEM images showed the generation of a large amount of geopolymer products by the reaction of OH– with the aluminosilicate components of the RHA in an alkaline source [77], most of the RHA particles reacted and bonded with the aggregate, and a gel was evident as confirmed by XRD analysis [78]
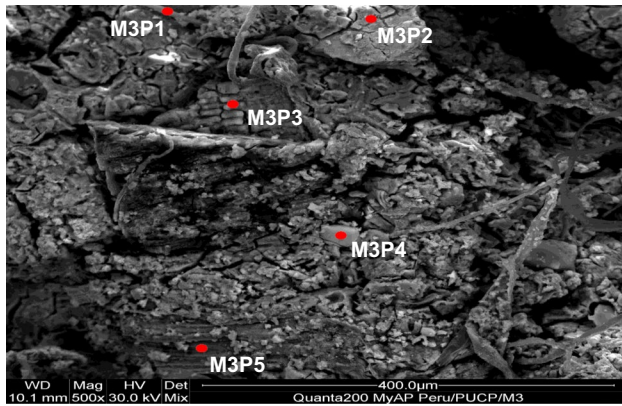

Fig. 27 Micrograph of sample M3—"Geopolymer chunks with 20% gypsum + 1.5% ichu + 1.5% ichu" at 400× with regions of interest indicated. *Source*: Authors
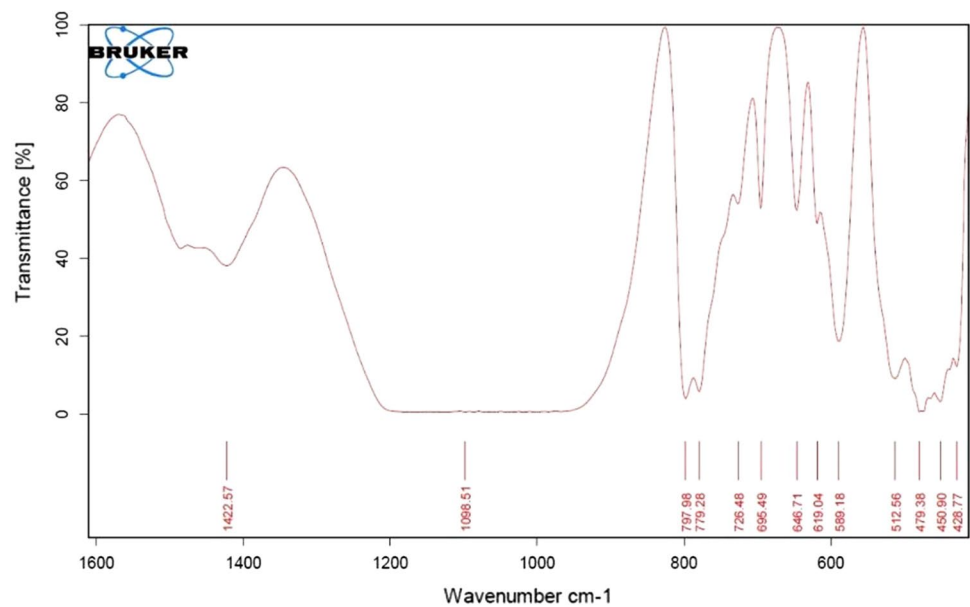
Fourier transform infrared (FTIR) spectroscopy: "Geopolymer with 20% gypsum + 1.5% ichu"

The FTIR analysis was performed on the geopolymer with the highest mechanical resistance, in this case the geopolymer with 20% gypsum and 1.5% ichu fiber. FTIR analysis was performed according to ASTM E1252-21 [71], Fig. 28 shows the FTIR spectrum of the geopolymer with the optimum molarity (12 Molar), optimum percentage of gypsum (20% gypsum), with the optimum mixed and at 1. 5% of ichu fiber, A Tensor 27 FTIR Infrared Spectrometer was used, with KBr pellet, The sample was ground and mixed with KBr in 20:1 ratio (KBr: Geopolymer), treated as indicated in ASTM E1252-21. It was identified that the analyzed peaks are compatible with geopolymers. FTIR spectra of the reference geopolymer specimens' evidence broad bands around 3450 cm^{-1} associated with O–H and H–O–H stretching vibrations. H–O–H bending vibrations are evident in the spectra near 1640 cm^{-1} from the chemically bonded water in the ge [79]. The most characteristic band is evident between 900 and 1100 cm^{-1}, it can be imputed to the presence of asymmetric stretching vibrations of Si–O–Si and Al–O–Si, which are the basic components of the geopolymer, and this range is lower than that of the C–A–S–H gel (i.e., 940 cm^{-1}) and higher than that of the N–A–S–H gel (i.e., 1030 cm^{-1}), which explains the evidence of several gel products [79, 80]. The peak around 793 cm^{-1} can be referred to symmetric Si–O–Si stretching vibrations. Si–O–Si and O-Si–O bending vibrations are related to the peaks around 450 and 480 cm^{-1} associated with the formation of sialate bonds (Si–O–Al–O) associated with the polycondensation of sodium silicate, this band is peculiar to crystalline cristobalite [34, 81]. However, the absorption peak was weak, which may be the result of carbonization during sample preparation [79].

Table 12 Chemical composition measured by EDS in various regions of interest of sample M3—"Geopolymer chunks with 20% gypsum + 1.5% ichu." *Source*: Authors

Chemical element	Total area		M3P1		M3P2		M3P3		M3P4		M3P5	
	wt%	at%	wt%	at%	wt%	at%	wt%	at%	wt%	at%	wt%	at%
C	23.40	35.47	35.61	47.82	–	–	39.34	57.10	–	–	–	–
O	39.09	42.66	35.52	35.81	38.71	55.64	19.34	21.07	33.17	51.07	44.39	60.44
Na	6.64	5.04	5.55	3.89	6.18	6.18	2.82	2.14	5.44	5.83	5.21	4.94
Mg	–	–	–	–	1.66	1.57	–	–	–	–	–	–
Al	1.18	0.77	3.22	1.92	6.41	5.46	–	–	–	–	1.10	0.89
Si	18.09	11.25	13.14	7.55	25.74	21.07	12.98	8.06	7.76	6.81	27.86	21.61
S	2.12	1.15	1.27	0.64	0.92	0.66	3.19	1.73	18.16	13.95	4.64	3.15
Cl	0.31	0.15	0.75	0.34	0.14	0.09	–	–	–	–	0.19	0.12
K	5.99	2.68	4.75	1.96	4.79	2.81	17.03	7.59	35.47	22.34	10.79	6.01
Ca	1.33	0.58	0.18	0.07	0.84	0.48	5.31	2.31	–	–	3.72	2.02
Mn	–	–	–	–	0.99	0.41	–	–	–	–	–	–
Fe	0.84	0.26	–	–	13.64	5.61	–	–	–	–	2.10	0.82

Fig. 28 FTIR spectrum of the pulverized geopolymer sample, showing the peaks identified and analyzed. *Source*: Authors

Thermogravimetric analysis (TGA): "Geopolymer with 20% gypsum + 1.5% ichu"

The thermogravimetric analysis was performed on the geopolymer with the highest mechanical resistance, in this case the geopolymer with 20% gypsum and 1.5% ichu fiber. From the thermogravimetric (TG) curve in Fig. 22 (blue and red curve), four mass change events are observed related to the decomposition of water and organic materials occurring before 600 °C and subsequently the decomposition of inorganic compounds in the presence of oxygen up to 990 °C. The residual mass at the end of the test at 990 °C is 90.6%. Likewise, the temperatures of maximum mass loss of water and organic materials 85, 160 and 274 °C (DTG, green curve in Fig. 23) and the decomposition of inorganic materials in the presence of oxygen at 611 and 940 °C are identified. Water evaporation and dihydroxylation are probably the consequences of mass loss during the heat treatment of the geopolymer [81]. The physical and chemical water of hardened geopolymers evaporates around 100 °C, and the chemical water between 100 and 300 °C, respectively.

At temperatures above 300 °C, the hydroxyl groups would gradually evaporate. At a temperature above 800–850 °C, the formation of a ceramic compound would begin [82]. Little mass loss above 800–850 °C would indicate the halt of further thermal decomposition of the geopolymer samples [83, 84]. The residual mass of the sample is 90.6%, with a total mass loss of 9.4%. [85]. The values of the results are presented in Table 13 and Fig. 29.

Conclusions

Taking into account the results and discussions, the following conclusions can be drawn:

The optimum calcination temperature of the rice RHA was 700 °C, which applying the ASTM C618 standard improving the strength by 10.2% with respect to the standard mortar of 21 MPa.
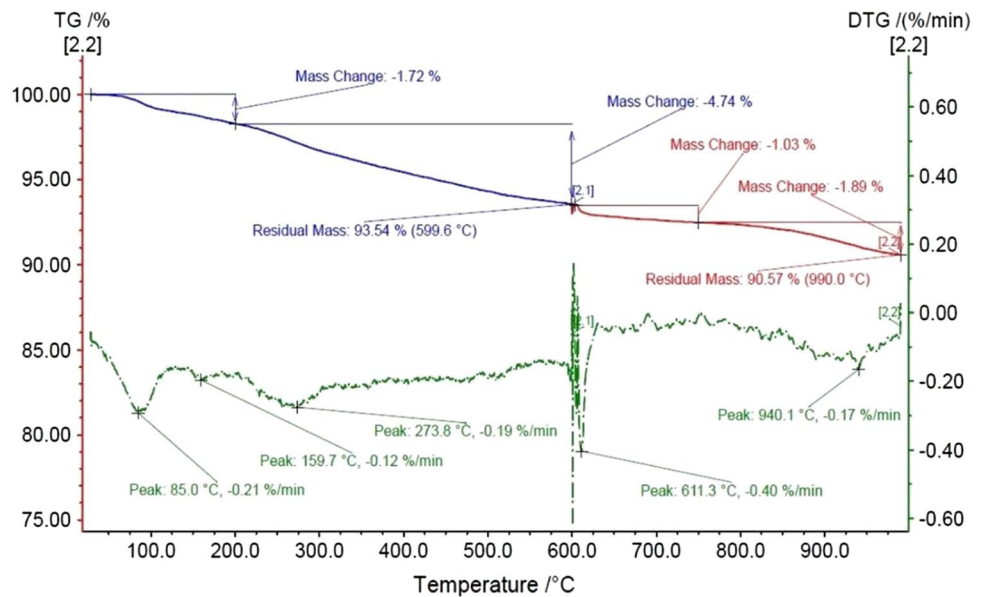
The 28-day compressive strength of the geopolymer with only RHA increases each time the molarity of sodium hydroxide increases up to 12 M, reaching a compressive

Table 13 Results of thermogravimetric analysis (TGA)

Sample	Maximum mass loss temperatures (*) (°C)	Loss of mass (%)				Residual mass a 990 °C (%)
		30–200 °C	200–600 °C	600–750 °C (**)	750–990 °C (**)	
Geopolymer	85	1.7	4.7	1.0	1.9	90.6
	160					
	274					
	611					
	940					

*From the DTG curve, **In oxygen environment

Fig. 29 Thermogram of the sample Powdered Geopolymer, Thermogravimetric Analysis (TGA—blue and red line) Derived from mass loss (DTG—green line). *Source*: Authors

strength of 2.34 MPa, and the compressive strength decreases if the molarity is higher than 12 M.

Geopolymer 12M20G achieved the best compressive strength at 28 days of 8.01 MPa and mix process A is the most optimal generating a compressive strength of 9.72 MPa; however, mix process C was the most optimal for flexural and tensile strengths of 3.24 and 2.36 MPa, respectively.

Geopolymer 12M20G1.5IF achieved the best flexural and tensile compressive strengths of 12.52, 7.99 and 2.25 MPa, respectively, showing that ichu fiber improves the mechanical properties of geopolymer.

In the geopolymer samples, mostly quartz and aluminosilicates were found, and those mixed with gypsum and ichu contain aphthalite, which is a form of gypsum commonly found in guano. Additionally, there is an appreciable percentage of amorphous material that cannot be identified by XRD. In the "rice husk ash" sample, two types of silicon oxide and a significant value of amorphous material were found.

The samples were analyzed by scanning electron microscopy (SEM) in conjunction with energy dispersive X-ray spectroscopy (EDS). The presence of carbon-rich inclusions, probably from plant-derived ash, was observed, which is consistent with the inclusion of rice husk ash. The presence of potassium, sodium and sulfur was also seen, suggesting the presence of gypsum in the samples that mention it. This is corroborated by XRD results.

A residual mass percentage of 90 6% is reached at 990 °C, and the geopolymer possesses O–H and H–O–H stretching vibrations, H–O–H bending vibrations in the spectrum near $1640 \ cm^{-1}$ and asymmetric Si–O–Si and Al–O–Si stretching vibrations, which are the basic elements of the geopolymer.

A geopolymer was developed using RHA as a precursor material, and with the addition of gypsum plus ichu fiber, reducing setting time and increasing mechanical strength. With the use of RHA as an input to develop geopolymers, environmental pollution can be reduced, since the use of cement would reduce the amount of cement used in the development of geopolymers.

Declarations

Conflict of interest The authors have no conflict of interest.

Ethical approval The article has not been submitted to more than one journal, is an original work with new findings presented in the article, has not been submitted elsewhere in any form or language.

Informed consent Formal consent is not required for this type of research.

References

1. Tun TZ, Bonnet Ś, Gheewala SH (2021) Emission reduction pathways for a sustainable cement industry in Myanmar. Sustain Prod Consum 27:449–461
2. Ali M, Sidur R, Hossain M (2011) A review on emission analysis in cement industries. Renew Sust Energ Rev 15(5):2252–2261

3. Torres M, Puertas F (2017) La activación alcalina de diferentes aluminosilicatos como una alternativa al Cemento Portland: cementos activados alcalinamente o geopolímeros. Rev Ing Constr 32(2):05

4. Shehata N, Sayed ET, Abdelkareem MA (2021) Recent progress in environmentally friendly geopolymers: a review. Sci Total Environ 762:143166

5. Babaee M, Castel A (2016) Chloride-induced corrosion of reinforcement in low-calcium fly ash-based geopolymer concrete. Cem Concr Res 88:96–107

6. Nguyen HT (2021) Microstructure stability and thermal resistance of ash-based geopolymer with sodium silicate solution at high temperature. Int J Eng Res Afr 53:101–111

7. Han Y, Lin R, Wang X (2021) Performance and sustainability of quaternary composite paste comprising limestone, calcined Hwangtoh clay, and granulated blast furnace slag. J Build Eng 43:102655

8. Sharma K, Kumar A (2022) Investigation of compaction, specific gravity, unconfined compressive strength and cbr of a composite having copper slag and rice husk ash mixed using an alkali activator. Innov Infrastruct Solut 7:185

9. Chokkalingam P, El-Hassan H, El-Dieb A (2022) Development and characterization of ceramic waste powder-slag blended geopolymer concrete designed using Taguchi method. Constr Build Mater 349:128744

10. Choeycharoen P, Sornlar W, Wannagon A (2022) A sustainable bottom ash-based alkali-activated materials and geopolymers synthesized by using activator solutions from industrial wastes. J Build Eng 54:104659

11. Kathirvel P, Sreekumaran S (2021) Sustainable development of ultra high performance concrete using geopolymer technology. Rev Ing Constr 39:102267

12. Verma M, Dev N, Rahman I, Nigam M, Ahmed M, Mallick J (2022) Geopolymer concrete: a material for sustainable development in Indian construction industries. Crystals 12(4):514

13. Somna R, Saowapun T, Somna K, Chindaprasirt P (2022) Rice husk ash and fly ash geopolymer hollow block based on NaOH activated. Case Stud Constr Mater 16:e01092

14. Kumar Das S, Adediran A, Rodrigue Kaze C, Mohammed Mustakim S, Leklou N (2022) Production, characteristics, and utilization of rice husk ash in alkali activated materials: an overview of fresh and hardened state properties. Constr Build Mater 345:128341

15. Mahdi SN, Hossiney N, Abdullah MM (2022) Strength and durability properties of geopolymer paver blocks made with fly ash and brick kiln rice husk ash. Case Stud. Constr. Mater. 16:e00800

16. Pham VP, Tran VT (2020) Rice husk ash burnt in simple conditions for soil stabilization. Geotech Sustain Infrastruct Dev Lect Notes Civ Eng 62:717–721

17. Rithuparna R, Jittin V, Bahurudeen A (2021) Influence of different processing methods on the recycling potential of agro-waste ashes for sustainable cement production: a review. J Clean Prod 316:128242

18. Newaz Khan MN, Jamil MA, Karim MR (2015) Utilization of rice husk ash for sustainable construction: a review. Res J Appl Sci Eng Technol 9(12):1119–1127

19. Mohd Basri MS, Mustapha F, Mazlan N, Ishak MR (2021) Rice husk ash-based geopolymer binder: compressive strength, optimize composition, FTIR spectroscopy, microstructural, and potential as fire-retardant material. Polymers 13(24):4373

20. Yadav AK, Gaurav K, Kishor R, Suman SK (2017) Stabilization of alluvial soil for subgrade using rice husk ash, sugarcane bagasse ash and cow dung ash for rural roads. Int J Pavement Res Technol 10(3):254–261

21. Abd-Ali MS, Kadhim SJ (2020) Experimental study on influence of Iraqi rice husk ash as supplementary material on the performance of concrete. IOP Conf Ser Mater Sci Eng 870:012050

22. Mounika G, Baskar R, Sri Kalyana Rama J (2022) Rice husk ash as a potential supplementary cementitious material in concrete solution towards sustainable construction. Innov Infrastruct Solut 7:51

23. Öztürk O (2021) Engineering performance of reinforced lightweight geopolymer concrete beams produced by ambient curing. Struct Concr 23:2076

24. Alsaif A, Albidah A, Abadel A, Abbas H, Al-Salloum Y (2022) Development of metakaolin-based geopolymer rubberized concrete: fresh and hardened properties. Arch Civ Mech Eng 22(3):144

25. Topçu İB, Sofuoğlu T (2021) Properties of geopolymers produced with sugar press filter waste and fly ash under certain curing conditions. J Build Eng 44:102938

26. Tarekegn M, Getachew K, Kenea G (2022) Experimental investigation of concrete characteristics strength with partial replacement of cement by hybrid coffee husk and sugarcane bagasse ash. Adv Mater Sci Eng 5363766:2022

27. Kotop MA, El-Feky M, Alharbi YR, Abadel AA, Binyahya AS (2021) Engineering properties of geopolymer concrete incorporating hybrid nano-materials. Ain Shams Eng J 12(4):3641–3647

28. Saloni, Parveen, Lim YY, Pham TM, Jatin, Kumar J (2021) Sustainable alkali activated concrete with fly ash and waste marble aggregates: strength and durability studies. Constr Build Mater 283:122795

29. Lianasari A, Atmajayanti A, Efendi B, Sitidaon N (2015) Sifat mekanik beton geopolimer berbasis solid material abu terbang (fly ash) dan abu sekam padi (rice husk ash) dengan alkaline activator sodium silikat dan sodium hidroksida. E-J Univ Atma Jaya Yogyak. http://e-journal.uajy.ac.id/id/eprint/7451

30. Hossain SS, Roy PK, Bae C-J (2021) Utilization of waste rice husk ash for sustainable geopolymer: a review. Constr Build Mater 310:125218

31. Chao-Lung H, Trong-Phuoc H (2015) Effect of alkali-activator and rice husk ash content on strength development of fly ash and residual rice husk ash-based geopolymers. Constr Build Mater 101:1–9

32. Zabihi SM, Tavakoli H, Mohseni E (2018) Engineering and microstructural properties of fiber-reinforced rice husk-ash based geopolymer concrete. J Mater Civ Eng 30(8):04018183

33. Januar F, Monita O, Iskandar R (2016) Perancangan mortar geopolimer abu sekam. J Online Mhs Fak Tek Univ Riau 3(2):1–8

34. Handayani L, Aprilia S, Abdullah, Rahmawati C, Aulia TB, Ludvig P, Ahmad J (2022) Sodium silicate from rice husk ash and their effects as geopolymer cement. Polymers 14(14):2920

35. Rosyadi A (2021) Prototipe semen geopolimer berbasis fly ash tipe C dengan Pengaruh Substitusi Abu Limbah Sekam Padi. http://repository.its.ac.id/id/eprint/83825

36. Ilmiah R (2017) Pengaruh Penambahan Abu Sekam Padi Sebagai Pozzolan Pada Binder geopolimer menggunakan alkali aktifator sodium silikat (Na$_2$SiO$_3$) serta sodium hidroksida (NaOH). http://repository.its.ac.id/id/eprint/2962

37. Kallamalayil Nassar A, Kathirvel P (2023) Effective utilization of agricultural waste in synthesizing activator for sustainable geopolymer technolgy. Const Build Mater 362:129681

38. An Q, Pan H, Zhao Q, Du S, Wang D (2022) Strength development and microstructure of recycled gypsum-soda residue-GGBS based geopolymer. Constr Build Mater 331:127312

39. Cong P, Mei L (2021) Using silica fume for improvement of fly ash/slag based geopolymer activated with calcium carbide residue and gypsum. Constr Build Mater 275:122171

40. Gholampour A, Danish A, Ozbakkaloglu T, HeumYeon J, Gencel O (2022) Mechanical and durability properties of natural

fiber-reinforced geopolymers containing lead smelter slag and waste glass sand. Constr Build Mater 352:129043

41. Ramakrishna G, Sundararajan T (2019) Long-term strength and durability evaluation of sisal fiber composites. In: Durability and life prediction in biocomposites, fibre-reinforced composites and hybrid composites, pp 211–255

42. Matalkah F, Soroushian P, Balchandra A, Peyvandi A (2017) Characterization of alkali-activated nonwood biomass ash-based geopolymer concrete. J Mater Civ Eng 29(4):04016270

43. Yang X, Zhang Y, Lin C (2022) Microstructure analysis and effects of single and mixed activators on setting time and strength of coal gangue-based geopolymers. Gels 8(13):195

44. Mahmood A, Noman MT, Pechočiaková M, Amor N, Petrů M, Abdelkader M, Militký J, Sozcu S, Ul Hassan SZ (2021) Geopolymers and fiber-reinforced concrete composites in civil engineering. Polymers 13(13):2099

45. Correia EA, Torres SM, Alexandre ME, Gomes KC, Barbosa NP, Barros SD (2013) Mechanical performance of natural fibers reinforced geopolymer composites. Mater Sci Forum 758:139–145

46. Ranjithkumar M, Chandrasekaran P, Rajeshkumar G (2022) Characterization of sustainable natural fiber reinforced geopolymer composites. Polym Compos 43(6):3691–3698

47. ASTM C1602M (2006) Standard specification for mixing water used in the production of hydraulic cement concrete. ASTM International

48. ASTM C136 (2001) Standard test method for sieve analysis of fine and coarse aggregates. ASTM International

49. ASTM C29 (2017) Standard test method for bulk density ("Unit Weight") and voids in aggregate. ASTM International

50. ASTM C128 (2016) Standard test method for relative density (specific gravity) and absorption of fine aggregate. ASTM International

51. ASTM C127 (2016) Standard test method for relative density (specific gravity) and absorption of coarse aggregate. ASTM International

52. ASTM C566 (2019) Standard test method for total evaporable moisture content of aggregate by drying. ASTM International

53. ASTM C131 (2020) Standard test method for resistance to degradation of small-size coarse aggregate by abrasion and impact in the Los Angeles machine. ASTM International

54. ASTM C117 (2017) Standard test method for materials finer than 75-μm (No. 200) sieve in mineral aggregates by washing. ASTM International

55. Hossain SS, Roy PK, Chang-Jun B (2021) Utilization of waste rice husk ash for sustainable geopolymer: a review. Constr Build Mater 310:125218

56. ASTM C618 (2022) Standard specification for coal fly ash and raw or calcined natural Pozzolan for use in concrete. ASTM International

57. García CJ, Navarro A, Ramírez J (2015) Estudio del yeso tradicional y sus aplicaciones en la arquitectura del pallars sobirá. https://core.ac.uk/download/pdf/46111557.pdf

58. Gire Quispe A, Caceres Lupaca AG (2019) Evaluación de La Influencia del tratamiento superficial sobre el comportamiento mecánico de fibras de Ichu en biocompuestos a base de Pla. http://repositorio.unsa.edu.pe/handle/UNSA/11140

59. Mori S, Charca S, Flores E, Salvastrano H (2019) Physical and thermal properties of novel native Andean natural fibers. J Natl Fibers 18(4):475–491

60. Tenazoa C, Savastano H, Charca S, Quintana M, Flores E (2019) The effect of alkali treatment on chemical and physical properties of ichu and cabuya fibers. J Natl Fibers 18:923

61. Candiotti S, Mantari JL, Flores CE, Charca S (2020) Assessment of the mechanical properties of peruvian Stipa Obtusa fibers for their use as reinforcement in composite materials. Compos A 135:105950

62. ASTM C188 (2017) Standard test method for density of hydraulic cement. ASTM International

63. ASTM D3822, "Standard Test Method for Tensile Properties of Single Textile Fibers," ASTM International, 2020.

64. Teewara S, Mitzi F (2017) Effect of manufacturing process on the mechanisms and mechanical properties of fly ash-based geopolymer in ambient curing temperature. Mater Manuf Processes 32(5):461–467

65. Weather Spark (2022) https://es.weatherspark.com/s/19294/2/Tiempo-promedio-en-el-oto%C3%B1o-en-Chiclayo-Per%C3%BA#Figures-SolarEnergy

66. ASTM C39/C39M (2019) ASTM C39/C39M standard test method for compressive strength of cylindrical concrete specimens. ASTM International

67. ASTM C138/C138M (2017) ASTM C138/C138M standard test method for density (unit weight), yield, and air content (gravimetric) of concrete—eLearning course. ASTM International

68. ASTM C469/C469M (2021) Standard test method for static modulus of elasticity and Poisson's ratio of concrete in compression. ASTM International

69. ASTM C78 (2022) Standard test method for flexural strength of concrete (using simple beam with third-point loading). ASTM International

70. ASTM C496 (1996) Standard test method for splitting tensile strength of cylindrical concrete specimens. ASTM International

71. ASTM E1252-21 (2021) Standard practice for general techniques for obtaining infrared spectra for qualitative analysis. ASTM International

72. ASTM E1131 (2020) Standard test method for compositional analysis by thermogravimetry—TGA. ASTM International

73. Torres-Carrasco M, Puertas F (2017) Alkaline activation of different aluminosilicates as an alternative to Portland cement: alkali activated cements or geopolymers. Rev Ing Constr 32(2):5–12

74. Davidovits J (2005) Geopolymers inorganic polymeric new materials. J Therm Anal Calorim 37(8):1633–1656

75. Liew Y, Kamarudin H, Al Bakri AM, Bnhussain M, Luqman M, Khairul Nizar I, Ruzaidi C, Heah C (2012) Optimization of solids-to-liquid and alkali activator ratios of calcined kaolin geopolymeric powder. Constr Build Mater 37:440–451

76. da Silva Alves LC, dos Reis Ferreira RA, Bellini Machado L, de Castro Motta LA (2019) Optimization of metakaolin-based geopolymer reinforced with sisal fibers. Ind Crops Prod 139:111551

77. Bellum RR, Venkatesh C, Madduru SRC (2021) Influence of red mud on performance enhancement of fly ash-based geopolymer concrete. Innov Infrastruct Solut 6(4):215

78. Diab MA (2022) Enhancing class F fly ash geopolymer concrete performance using lime and steam curing. J Eng Appl Sci 69(1):59

79. Guo L, Zhou M, Wang X, Li C, Jia H (2022) Preparation of coal gangue-slag-fly ash geopolymer grouting materials. Constr Build Mater 328:126997

80. Zhang M, Zhao M, Zhang G, El-Korchi T, Tao M (2017) A multiscale investigation of reaction kinetics, phase formation, and mechanical properties of metakaolin geopolymers. Cement Concr Compos 78:21–32

81. Kljajević L, Nenadović M, Ivanović M, Bučevac D, Mirković M, Nikolić NM, Nenadović S (2022) Heat treatment of geopolymer samples obtained by varying concentration of sodium hydroxide as constituent of alkali activator. Gels 8(6):333

82. Redaoui D, Sahnoune F, Heraiz M, Raghdi A (2017) Mechanism and kinetic parameters of the thermal decomposition of gibbsite $Al(OH)_3$ by thermogravimetric analysis. Acta Phys Pol Ser 131(3):562–565

83. Elimbi A, Tchakoute HK, Kondoh M, Dika Manga J (2014) Thermal behavior and characteristics of fired geopolymers produced from local Cameroonian metakaolin. Ceram Int 40(3):4515–4520

84. Bayat A, Ooholamini H, Farahani M (2022) Effect of bauxite residue inclusion on the strength, shrinkage, and abrasion of alkali-activated slag concrete. Innov Infrastruct Solut 7:331

85. Yavuz E, Kul Gul NI (2022) Characterization of class C and F fly ashes based geopolymers incorporating silica fume. Ceram Int 48(21):32213–32225

Authors and Affiliations

Sócrates Pedro Muñoz Pérez[1,2] · **Samuel Charca Mamani[3]** · **Luigui Italo Villena Zapata[4]** · **Jorge Luis Leiva Piedra[5]** · **Simon Gonzales Ayasta[6]** · **Ernesto Dante Rodriguez Lafitte[6]** · **Fidel Gregorio Aparicio Roque[7]** · **Omar Coronado Zuloeta[8]**

✉ Sócrates Pedro Muñoz Pérez
   socrates.munoz@untrm.edu.pe; 2020812016@uns.edu.pe

Samuel Charca Mamani
scharca@utec.edu.pe

Luigui Italo Villena Zapata
vzapataluigiita@crece.uss.edu.pe

Jorge Luis Leiva Piedra
jleiva@utp.edu.pe

Simon Gonzales Ayasta
gayastasimon@crece.uss.edu.pe

Ernesto Dante Rodriguez Lafitte
rlafitte@crece.uss.edu.pe

Fidel Gregorio Aparicio Roque
daparicior@unasam.edu.pe

Omar Coronado Zuloeta
ocornado@unprg.edu.pe

[1] Graduate School, Doctorate in Civil Engineering, National University of Santa, 02712 Chimbote, Perú

[2] Faculty of Civil and Environmental Engineering, Academic and Professional School of Civil Engineering, Universidad Nacional Toribio Rodríguez De Mendoza De Amazonas, 01001 Chachapoyas, Perú

[3] Professional School of Mechanical Engineering, University of Engineering and Technology PrivateUniversity, 15011 Lima, Perú

[4] Professional School of Business Administration, School of Business Science, Universidad César Vallejo, Universidad César Vallejo, 13001 Trujillo, Perú

[5] School of Industrial Engineering, Technological University of Peru, 15046 Pimentel, Perú

[6] School of Engineering and Architecture, Professional School of Civil Engineering, Universidad Señor de Sipan, 14000 Pimentel, Perú

[7] Faculty of Agricultural Sciences, Professional School of Agricultural Engineering, Universidad Nacional Santiago Antúnez de Mayolo, 02002 Huaraz, Perú

[8] Faculty of Civil Engineering, Systems and Architecture, Professional School of Civil Engineering, Universidad Nacional Pedro Ruiz Gallo, 14013 Lambayeque, Perú